



Zero-chromatic FFAGs for muon acceleration

T. Planche, E. Yamakawa, J-B. Lagrange, T. Uesugi, Y. Kuriyama, Y. Ishi, Y. Mori: Kyoto University, Japan.
J. Pasternak : Imperial College London/RAL STFC, UK.

Motivations

Features of the **scaling type** of **fixed field alternating gradient** (FFAG) rings:

(i) free from resonance crossing issues, **large transverse acceptances** can be achieved once the working point is chosen far enough from harmful resonances;

(ii) free from the issue of time-of-flight dependence on the transverse amplitude^(*). This limits the **longitudinal emittance degradation** when beams with large transverse emittances are accelerated.

^(*) see S. Berg, Nucl. Instr. and Meth. A 570, p.~15, (2007).

Aim

Develop scaling FFAG lattices:

- (i) with $> 30 \pi$ mm-rad of normalized transverse acceptance for both horizontal and vertical plane, and > 150 mm of normalized longitudinal acceptance,
- (ii) using **200 MHz constant frequency** rf cavities
- (iii) to accelerate simultaneously μ^+ and μ^- beams.

Contents

- 1 - Acceleration inside a stationary rf bucket
- 2 - Example of 3.6 to 12.6 GeV muon ring parameters
- 3 - Tracking simulations
 - 3.1 - 4D & 6D tracking results
 - 3.2 - Study with errors
 - 3.3 - Preliminary beam injection/extraction (from J. Pasternak)
- 6 - Summary and discussions

Acceleration inside the stationary rf bucket of a scaling FFAG ring

Principle: use the synchrotron motion to accelerate beam going from the low energy to the high energy part of a stationary rf bucket.

Case of scaling FFAGs: since the momentum compaction is constant with energy, the longitudinal dynamics can be analytically described without

assuming $\frac{\Delta p}{p}$ small^(*).

^(*) see E.Yamakawa and Y. Mori's paper to appear in proceedings of FFAG'09 conference.

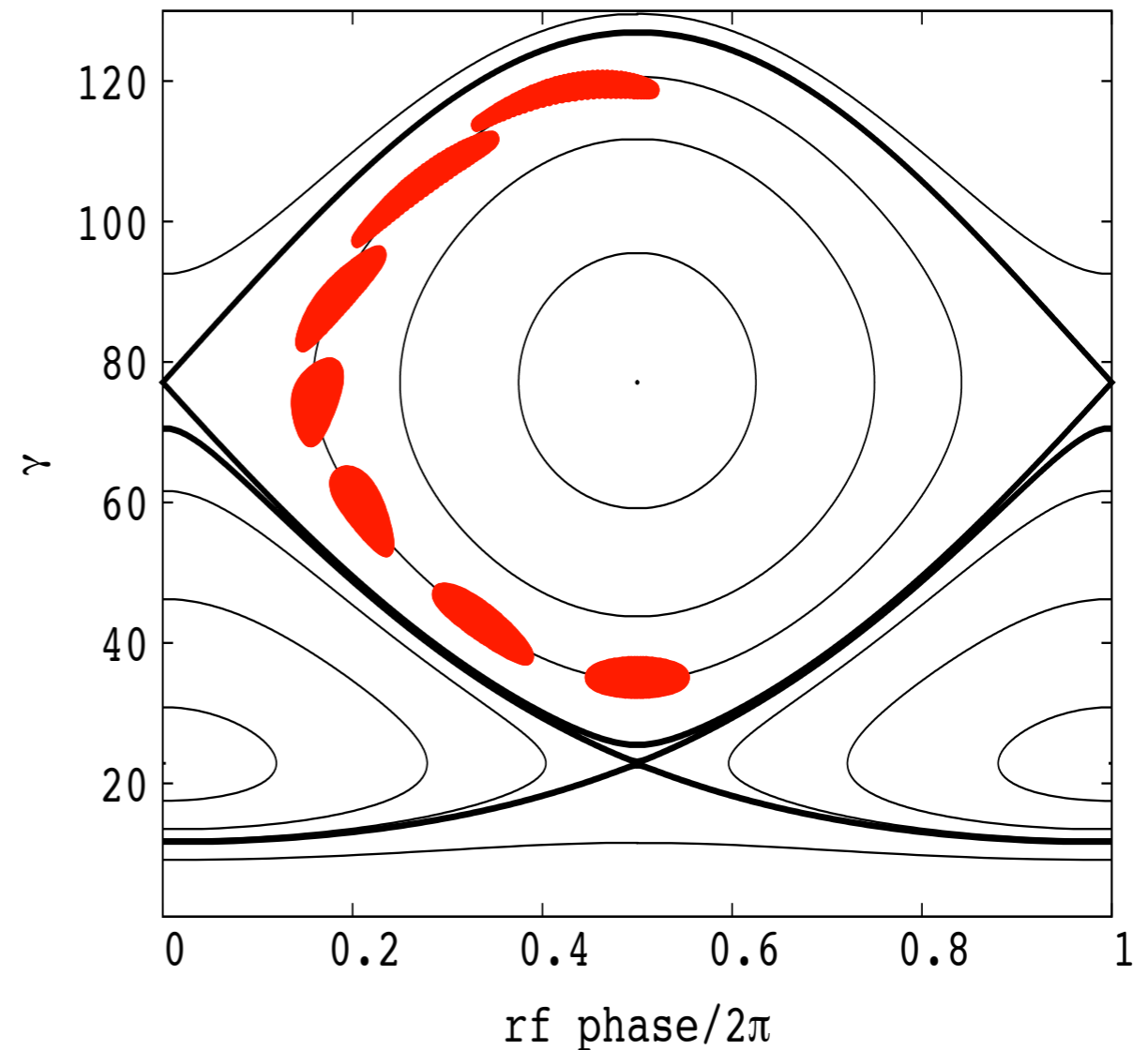


Figure 1 - Longitudinal phase space showing the acceleration of a muon beam (red) inside the stationary rf bucket of a scaling FFAG ring. Hamiltonian contours are shown in black.

Choice of the working point

Emittance scan in the case of a ring made of 225 identical FDF triplet FFAG cells. Legends in the top left corner of each diagram give values of acceptances normalized in the case of 3.6 GeV muons. Normal structure resonances lines, plotted up to the octupole, are superimposed.

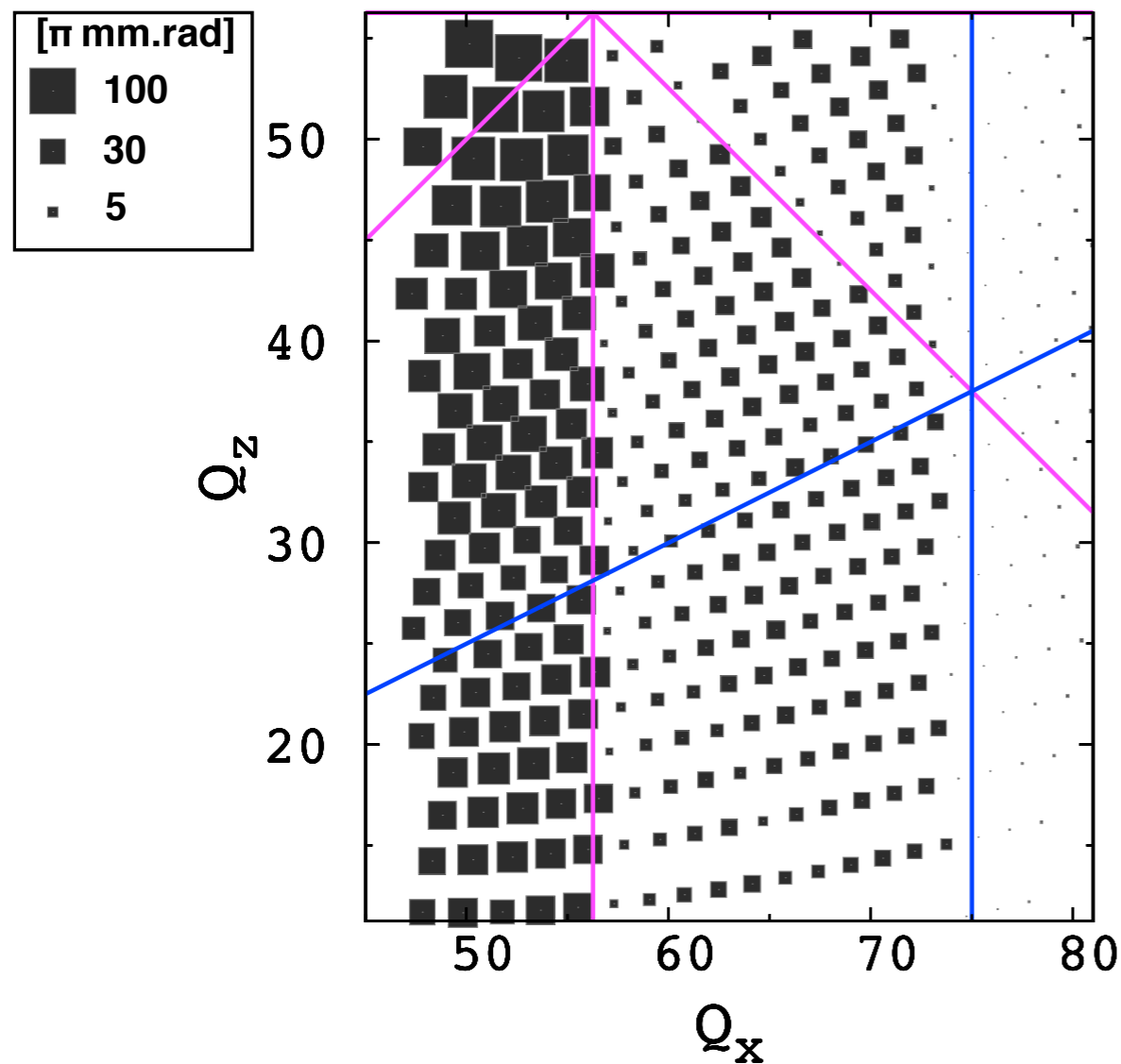


Figure 2a - Horizontal acceptance scan.

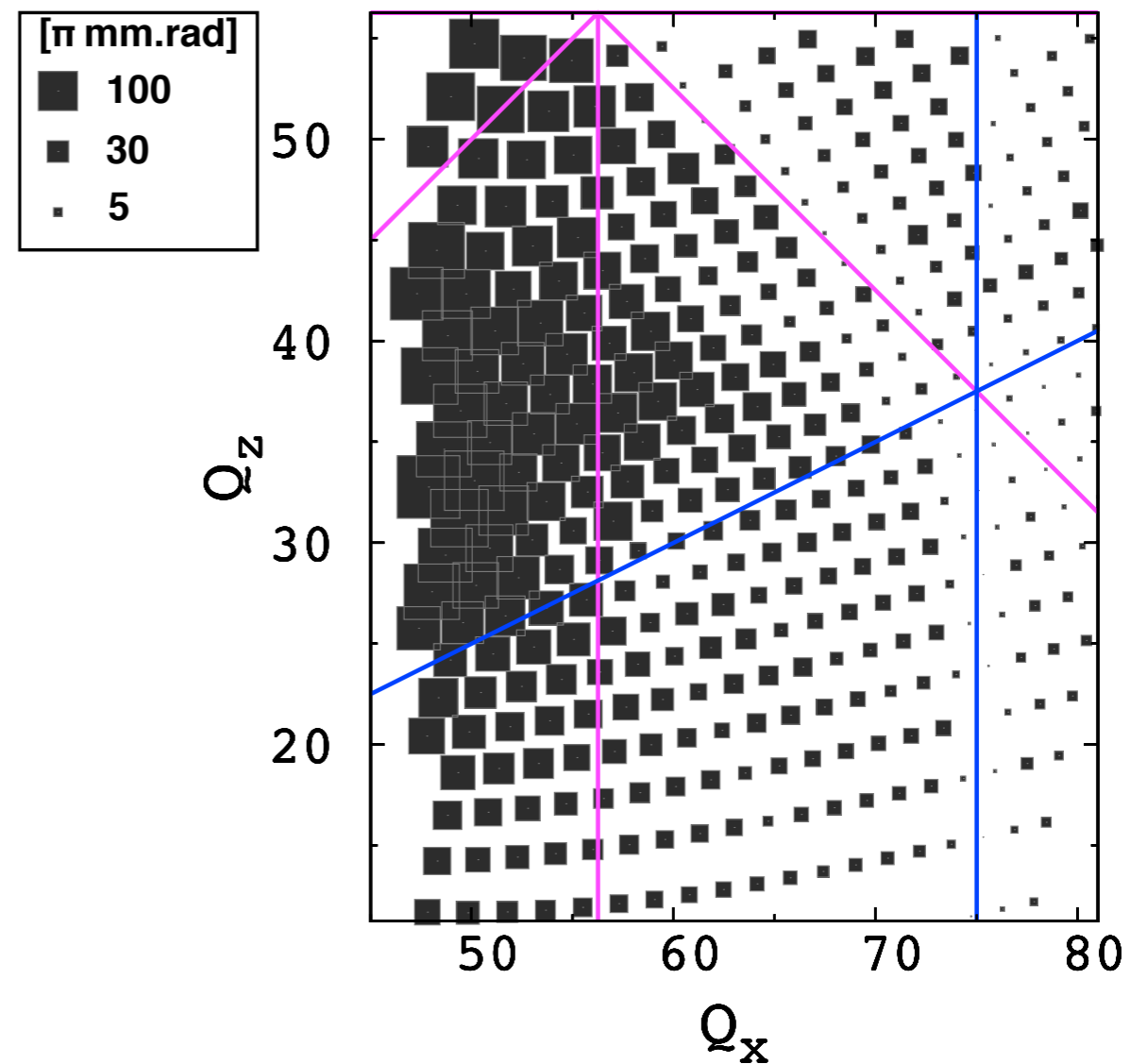


Figure 2b - Vertical acceptance scan.

Choice of the working point

Emittance scan in the case of a ring made of 225 identical FDF triplet FFAG cells. Legends in the top left corner of each diagram give values of acceptances normalized in the case of 3.6 GeV muons. Normal structure resonances lines, plotted up to the octupole, are superimposed.

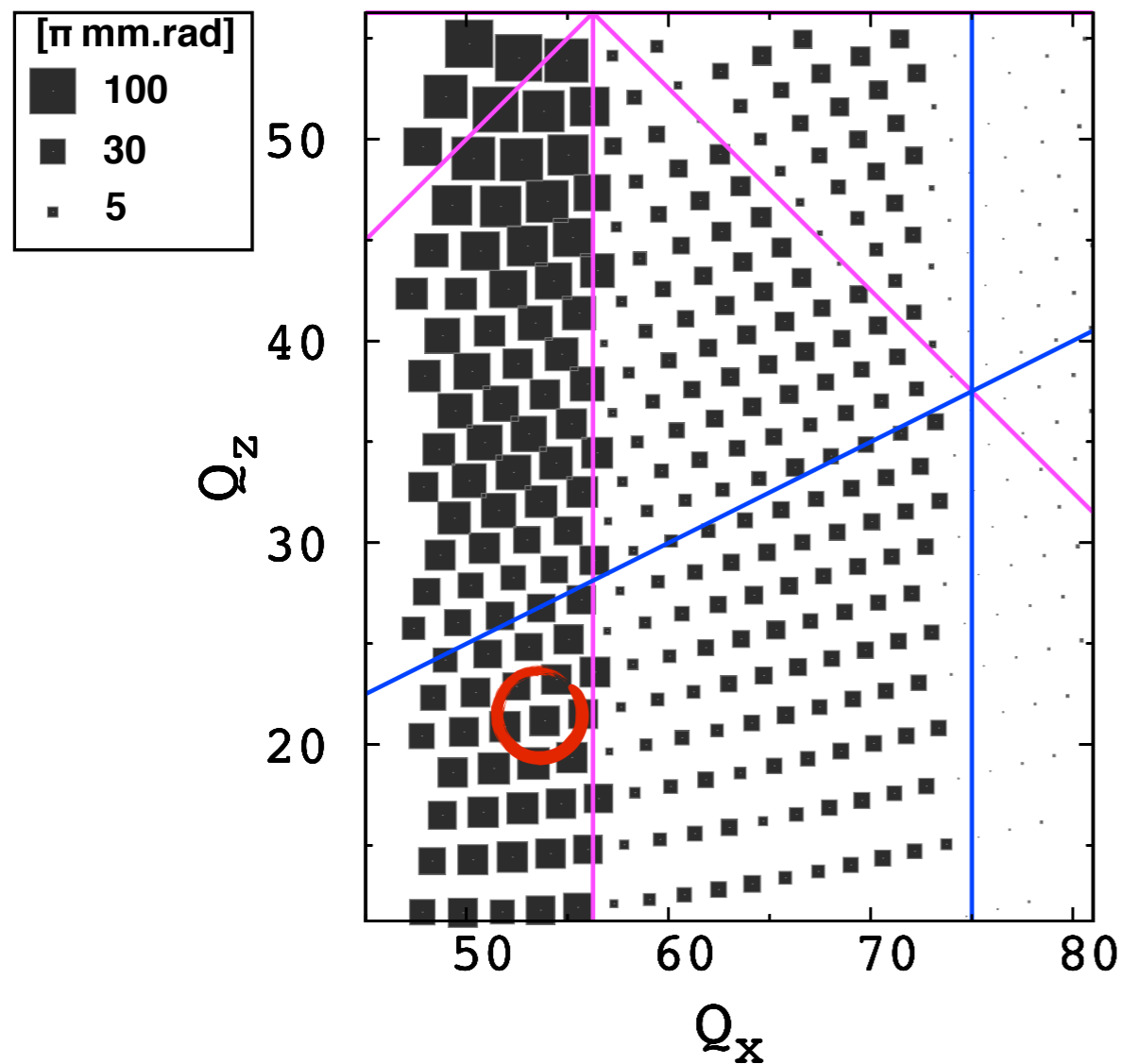


Figure 2a - Horizontal acceptance scan.

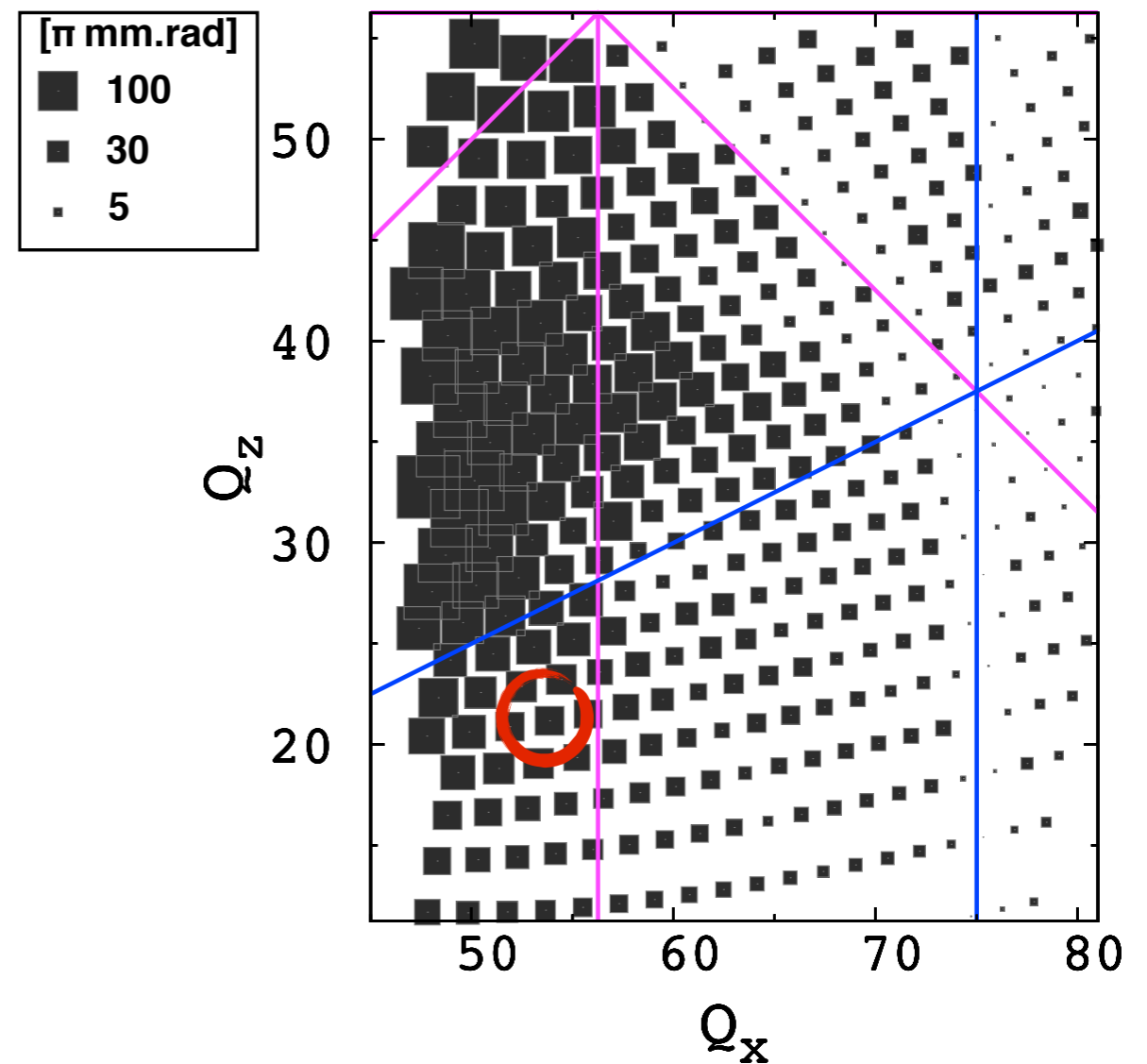


Figure 2b - Vertical acceptance scan.

Parameters of a 3.6 to 12.6 GeV muon ring

Lattice type	FDF triplet
Injection/extraction energy	3.6/12.6 GeV
RF frequency	200 MHz
Number of turns	6
RF peak voltage (per turn)	1.8 GV
Synchronous energy	8.04 GeV
Mean radius	~ 160.9 m
B_{max} (@ 12.6 GeV)	3.9 T
Field index k	1390
Total orbit excursion	14.3 cm
Harmonic number h	675
Number of cells	225
Long drift length	~ 1.5 m
Horiz. phase adv. per cell	85.86 deg.
Vert. phase adv. per cell	33.81 deg.

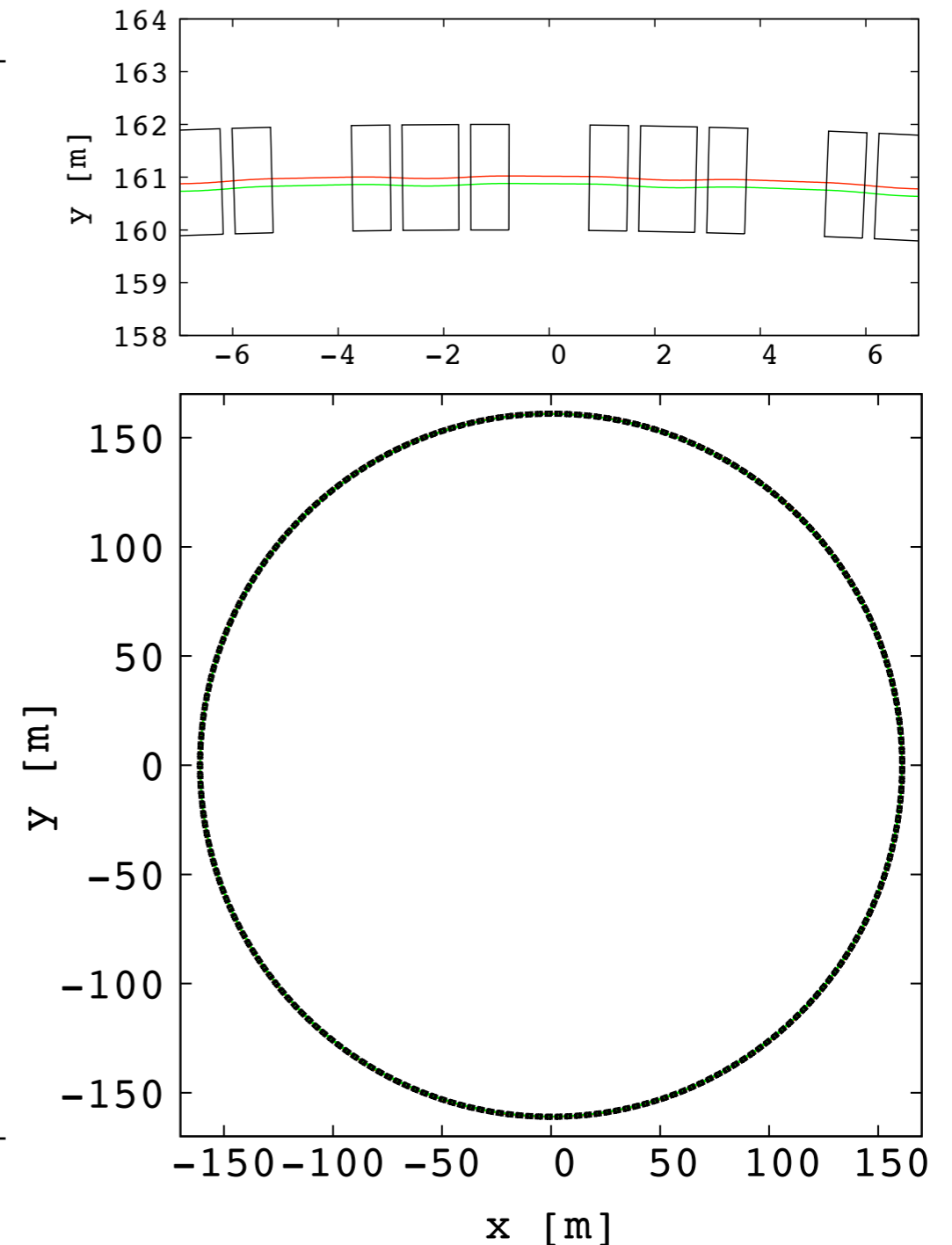


Figure 3 - Ring layout.

Table I - Example of 3.6 to 12.6 GeV muon scaling FFAG ring parameters.

Parameters of a 3.6 to 12.6 GeV muon ring

Lattice type	FDF triplet
Injection/extraction energy	3.6/12.6 GeV
RF frequency	200 MHz
Number of turns	6
RF peak voltage (per turn)	1.8 GV
Synchronous energy	8.04 GeV
Mean radius	~ 160.9 m
B_{max} (@ 12.6 GeV)	3.9 T
Field index k	1390
Total orbit excursion	14.3 cm
Harmonic number h	675
Number of cells	225
Long drift length	~ 1.5 m
Horiz. phase adv. per cell	85.86 deg.
Vert. phase adv. per cell	33.81 deg.

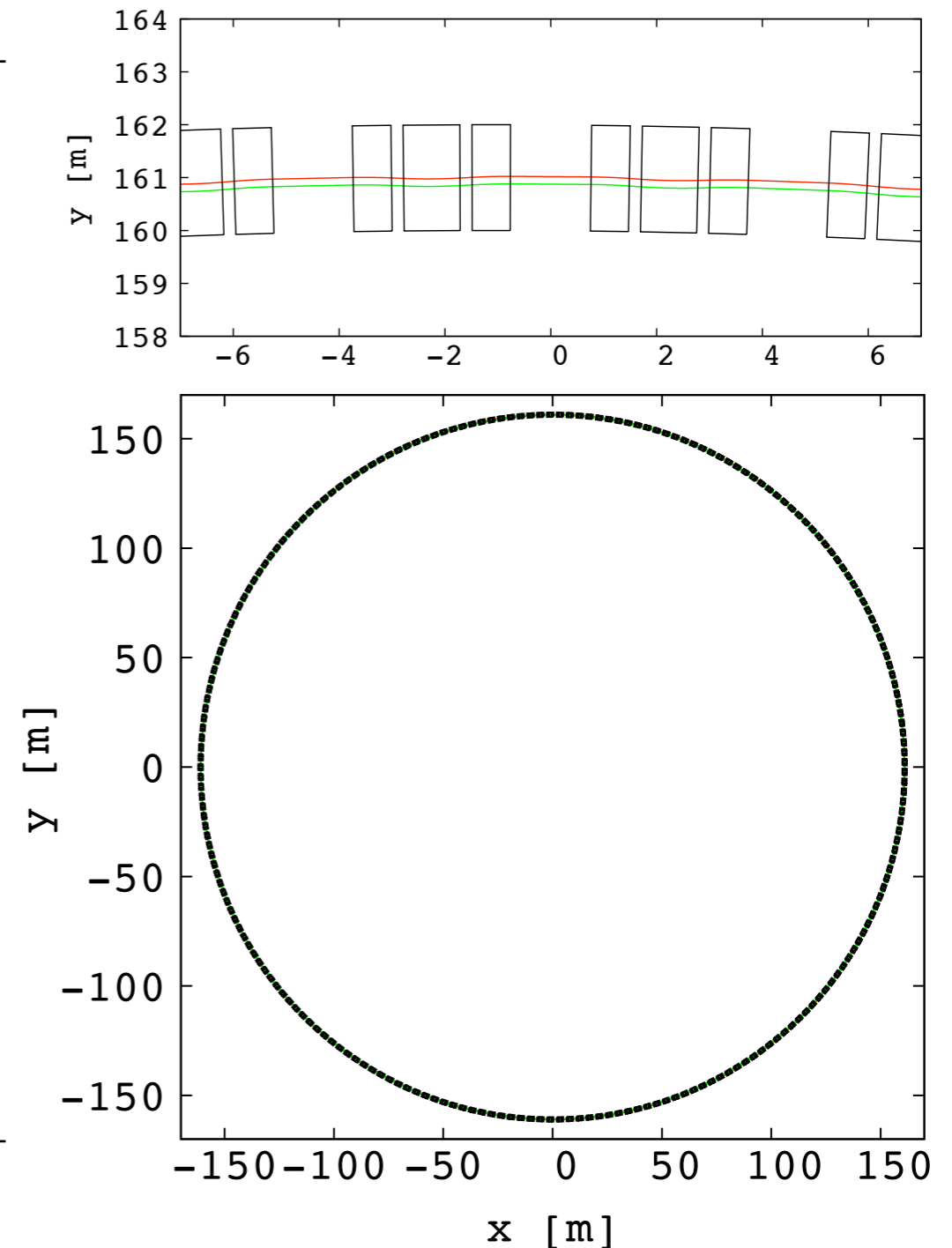


Figure 3 - Ring layout.

Table I - Example of 3.6 to 12.6 GeV muon scaling FFAG ring parameters.

Parameters of a 3.6 to 12.6 GeV muon ring

Lattice type	FDF triplet
Injection/extraction energy	3.6/12.6 GeV
RF frequency	200 MHz
Number of turns	6
RF peak voltage (per turn)	1.8 GV
Synchronous energy	8.04 GeV
Mean radius	~ 160.9 m
B_{max} (@ 12.6 GeV)	3.9 T
Field index k	1390
Total orbit excursion	14.3 cm
Harmonic number h	675
Number of cells	225
Long drift length	~ 1.5 m
Horiz. phase adv. per cell	85.86 deg.
Vert. phase adv. per cell	33.81 deg.

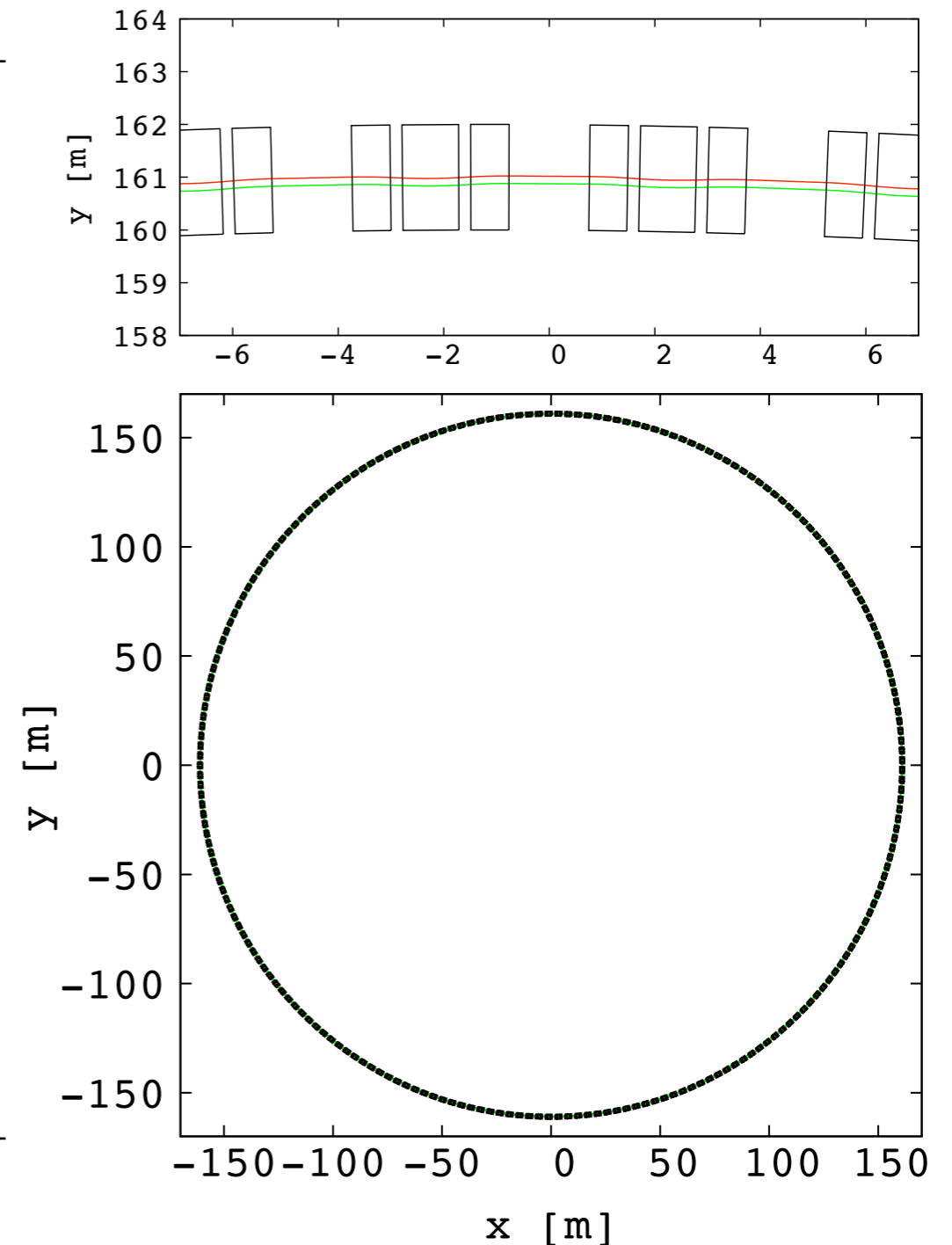


Figure 3 - Ring layout.

Table I - Example of 3.6 to 12.6 GeV muon scaling FFAG ring parameters.

Parameters of a 3.6 to 12.6 GeV muon ring

Lattice type	FDF triplet
Injection/extraction energy	3.6/12.6 GeV
RF frequency	200 MHz
Number of turns	6
RF peak voltage (per turn)	1.8 GV
Synchronous energy	8.04 GeV
Mean radius	~ 160.9 m
B_{max} (@ 12.6 GeV)	3.9 T
Field index k	1390
Total orbit excursion	14.3 cm
Harmonic number h	675
Number of cells	225
Long drift length	~ 1.5 m
Horiz. phase adv. per cell	85.86 deg.
Vert. phase adv. per cell	33.81 deg.

Table I - Example of 3.6 to 12.6 GeV muon scaling FFAG ring parameters.

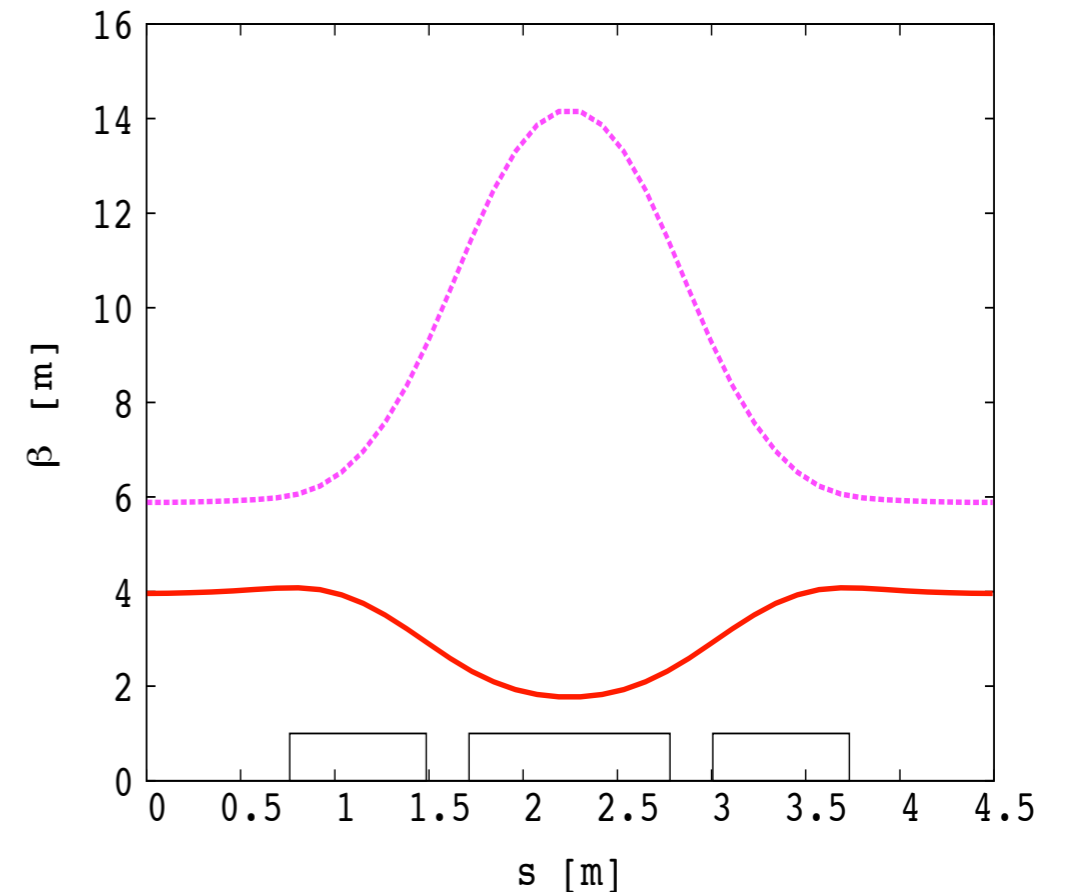
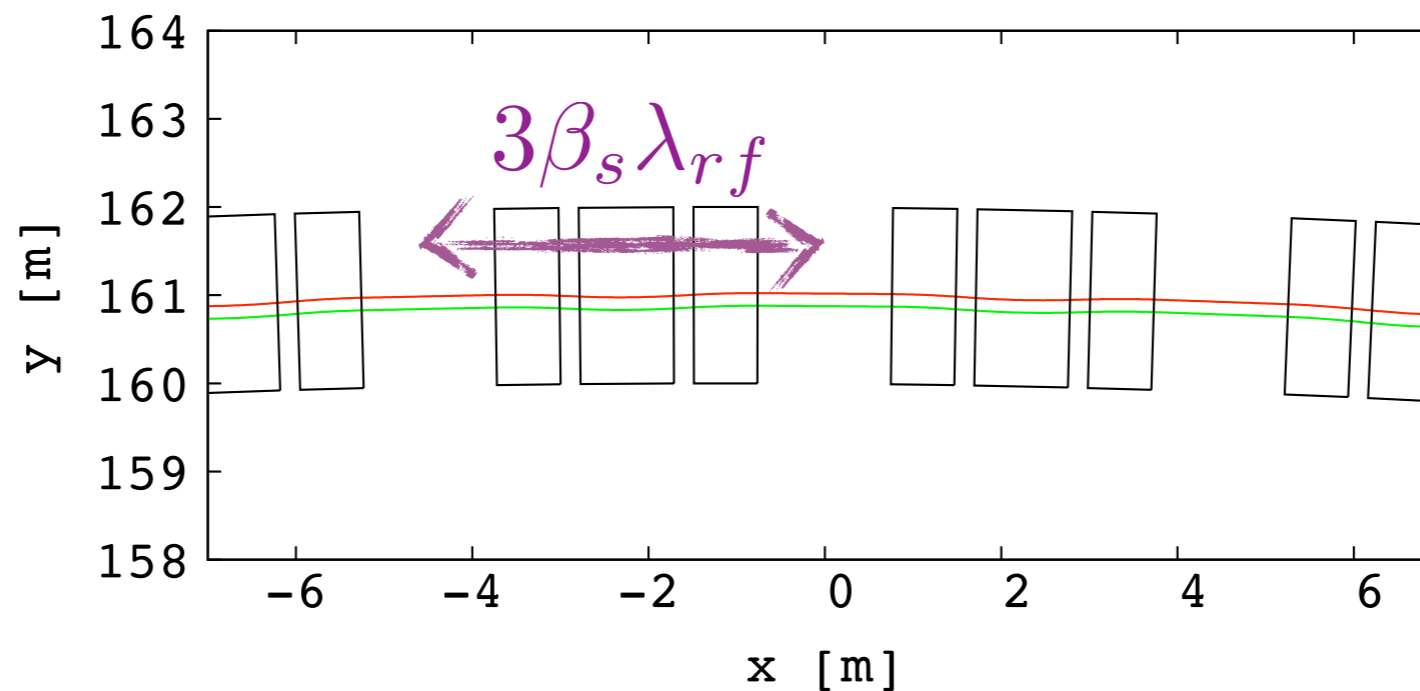


Figure 4 - Horizontal (red) and vertical (purple) beta function at 3.6 GeV, calculated using set-wise tracking in soft-edge field model from small amplitude motion around the closed orbit. Position of the magnets effective field boundaries are shown with rectangles.

Parameters of a 3.6 to 12.6 GeV muon ring

Simultaneous acceleration of μ^+ and μ^- beams:



In order to allow the simultaneous acceleration of μ^+ and μ^- beams, the synchronous particle orbit length is adjusted to a multiple of $\frac{1}{2}\beta_s\lambda_{rf}$.

Simulation tools

We use step-wise particle tracking in geometrical field model to determine the lattice linear parameters and study the beam dynamics.

Mid-plane field distribution follows:

$$B_z(r, \theta) = B_0 \left(\frac{r}{r_0} \right)^k \mathcal{F}(\theta).$$

The azimuthal field law $\mathcal{F}(\theta)$ is softened using Enge type of field fall-off.

Field off the mid-plane is obtained, following the Maxwell's equations, from a 4th order Taylor expansion.

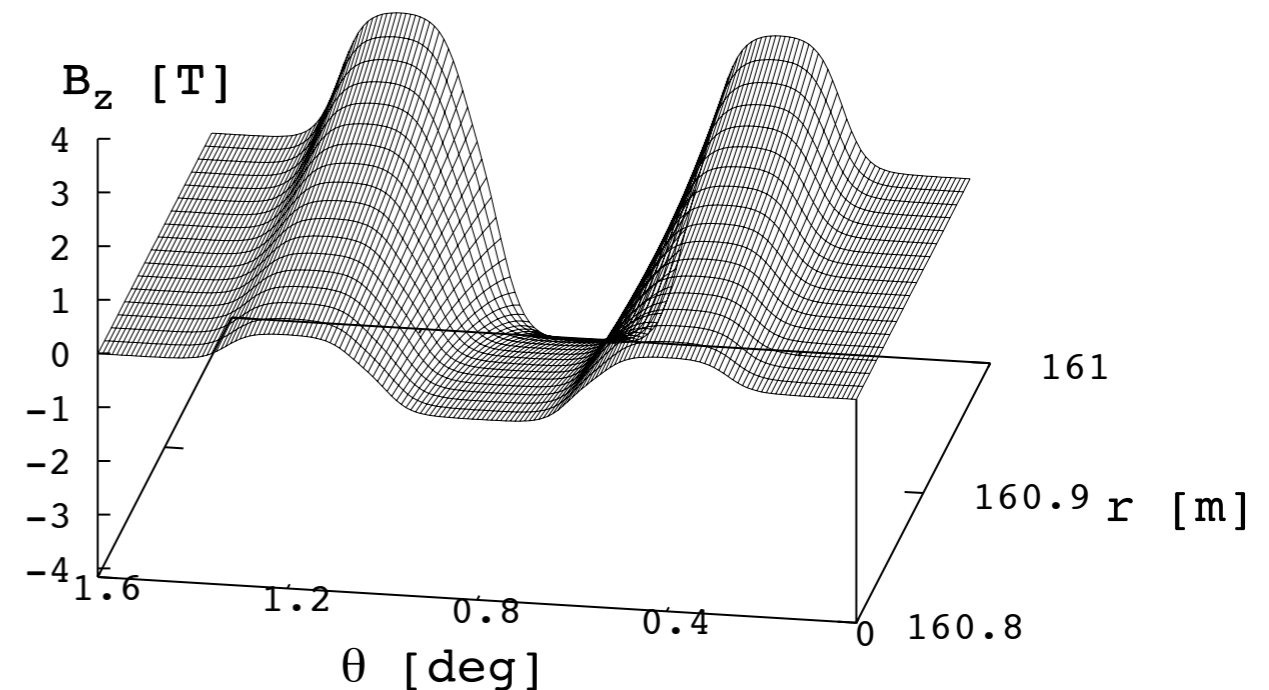
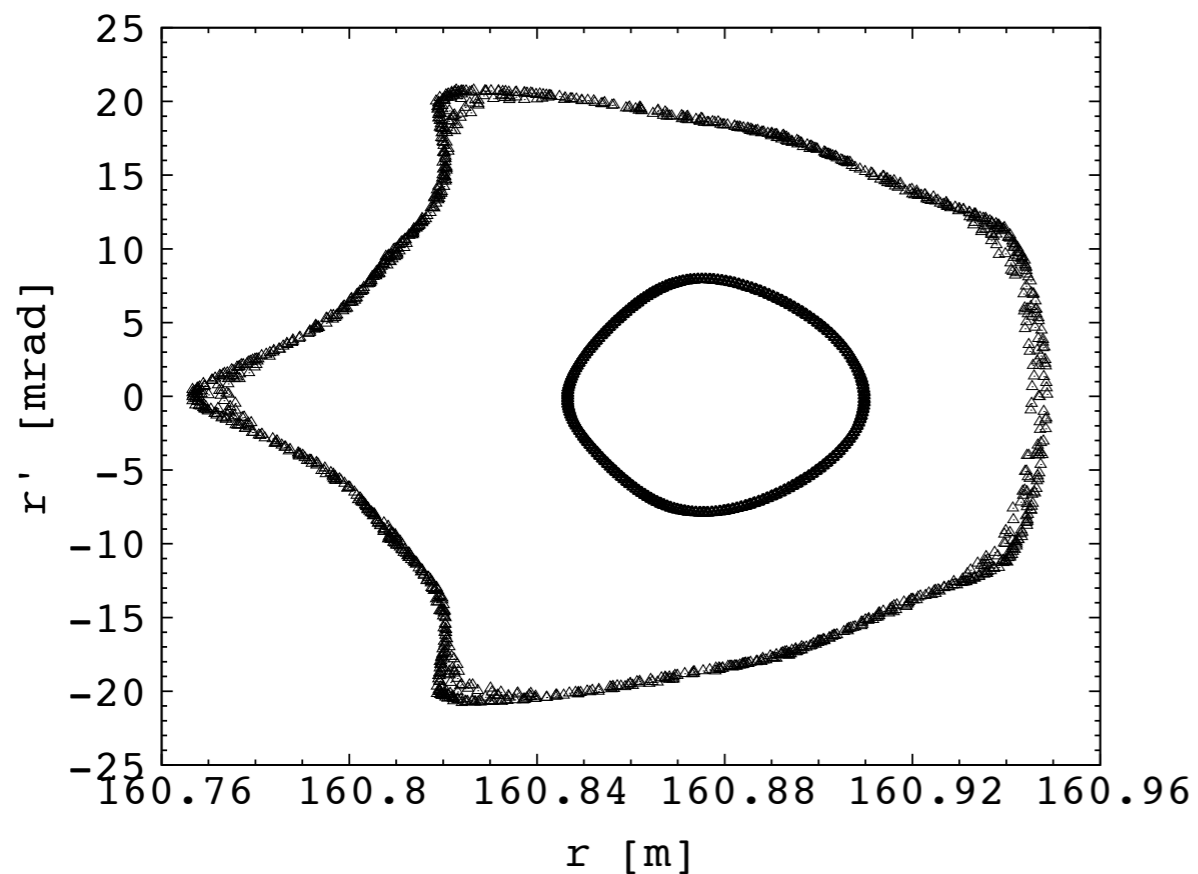


Figure 5 - Vertical B field distribution the mid-plane of a triplet cell.

Transverse acceptance at fixed energy

Horizontal acceptance $> 30 \pi$ mm-rad normalized at 3.6 GeV

Using a Runge-Kutta based tracking code (developed at Kyoto university)



Using 'FFAG' procedure of Zgoubi

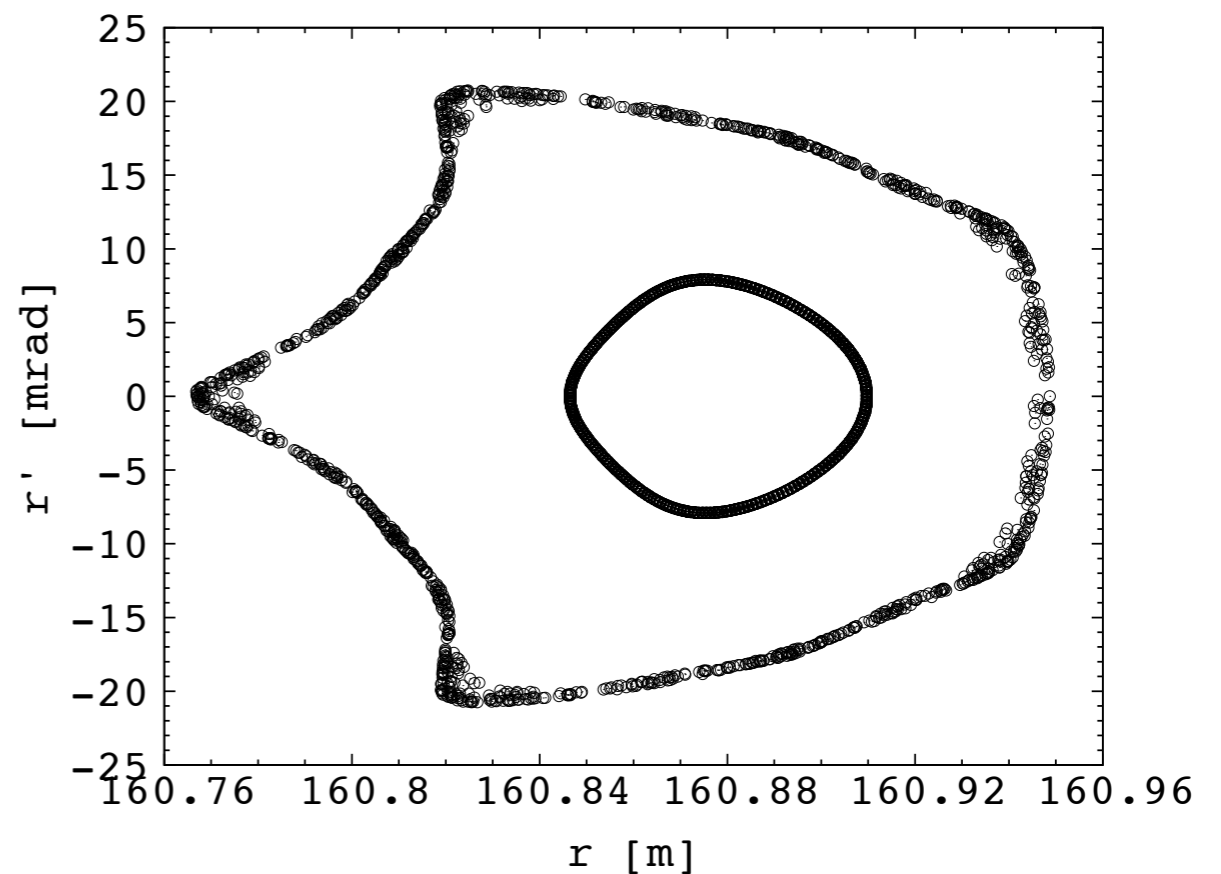
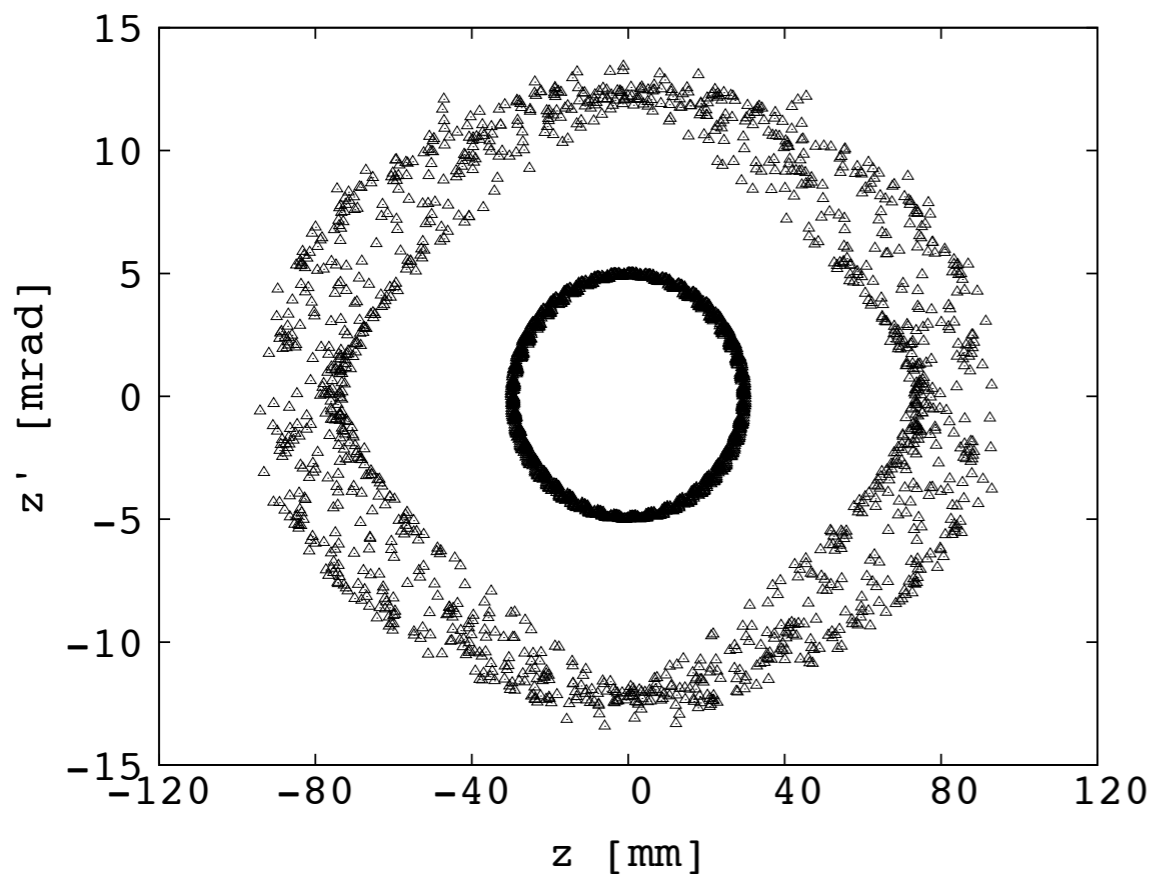


Figure 6 - (r, r') plane (@ middle of the long drift) showing a multi-turn tracking of 2 particles with different initial horizontal amplitudes, with an initial vertical displacement = 1 mm.

Transverse acceptance at fixed energy

Vertical acceptance is also $> 30 \pi$ mm-rad normalized at 3.6 GeV

Using a Runge-Kutta based tracking code (developed at Kyoto university)



Using 'FFAG' procedure of Zgoubi

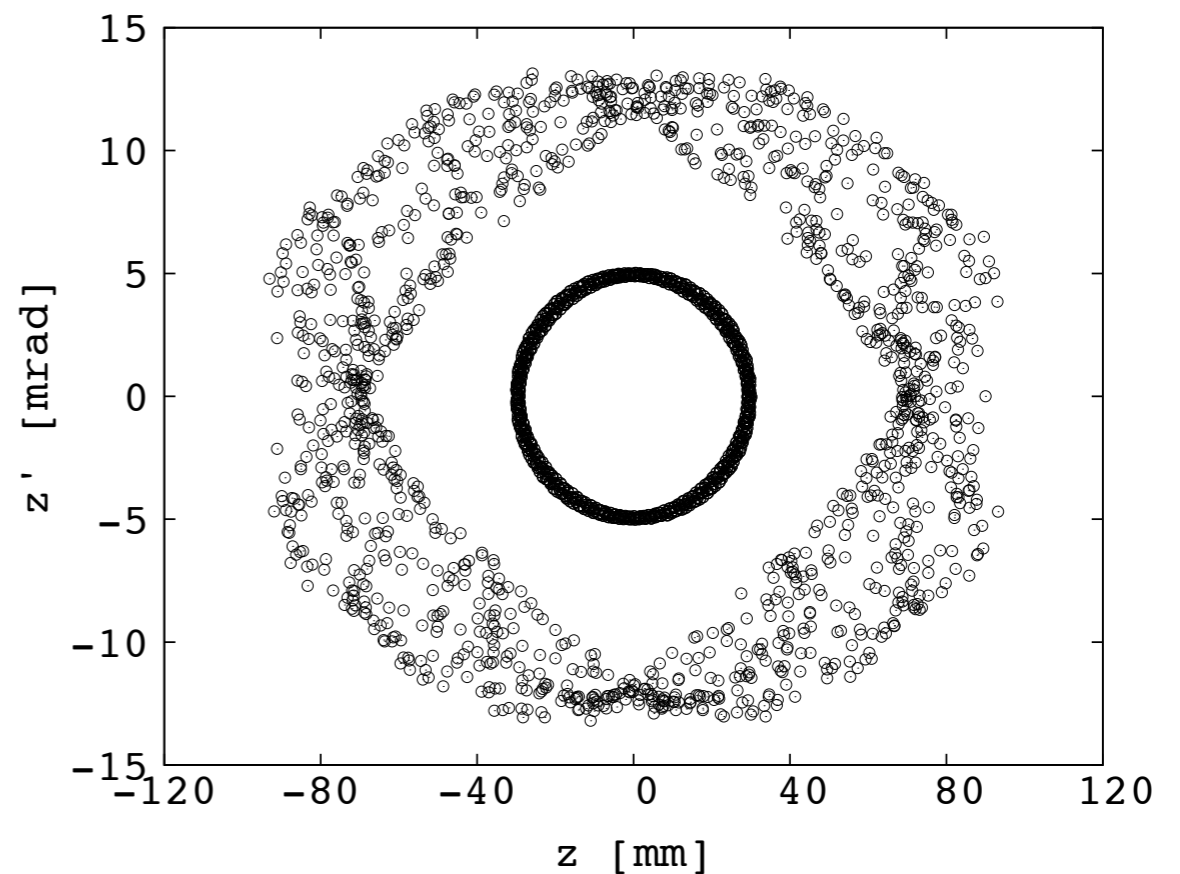


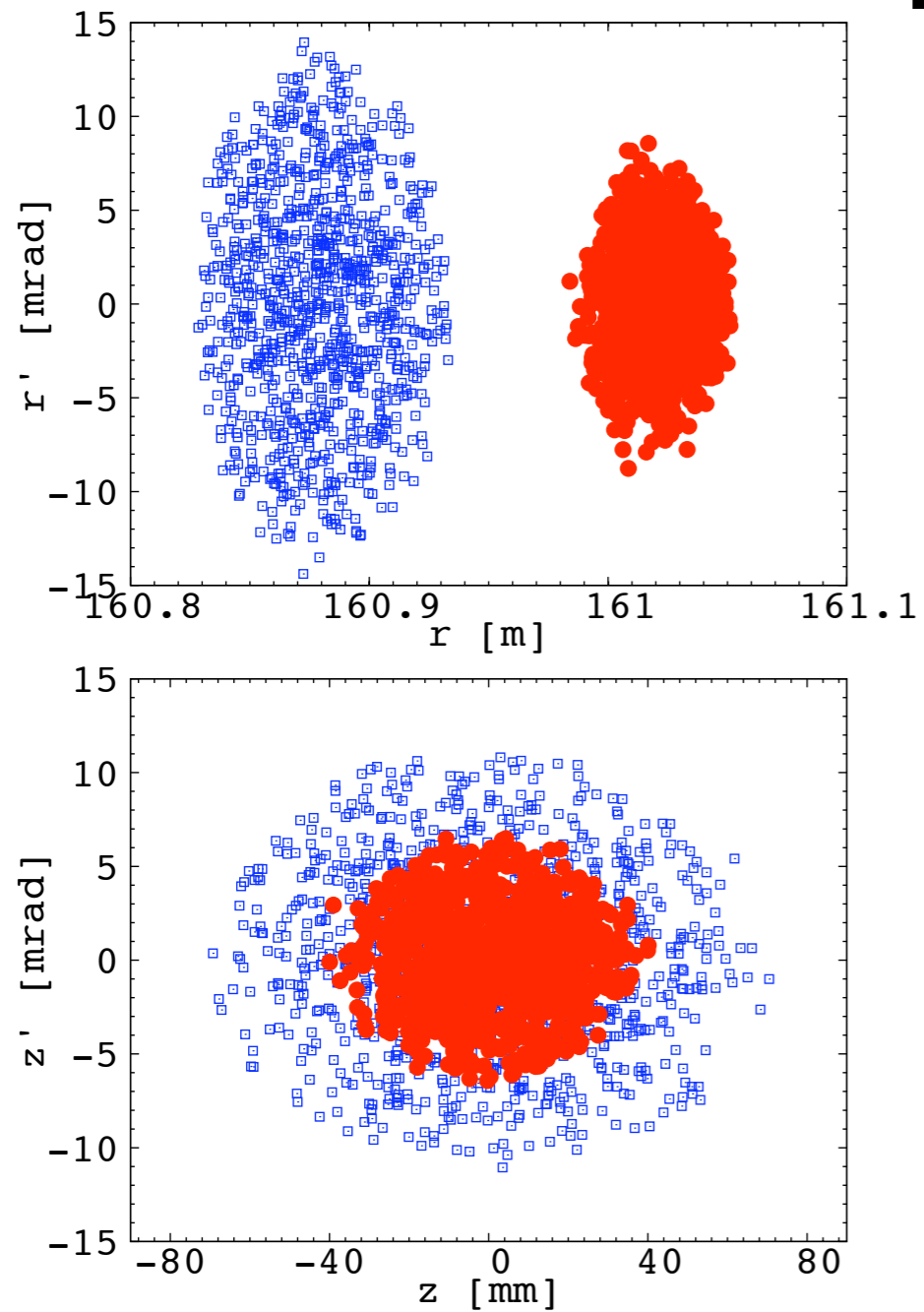
Figure 7 - (z, z') plane (@ middle of the long drift) showing a multi-turn tracking of 2 particles with different initial vertical amplitudes, with an initial horizontal displacement = 1 mm.

Full acceleration cycle - 6D tracking

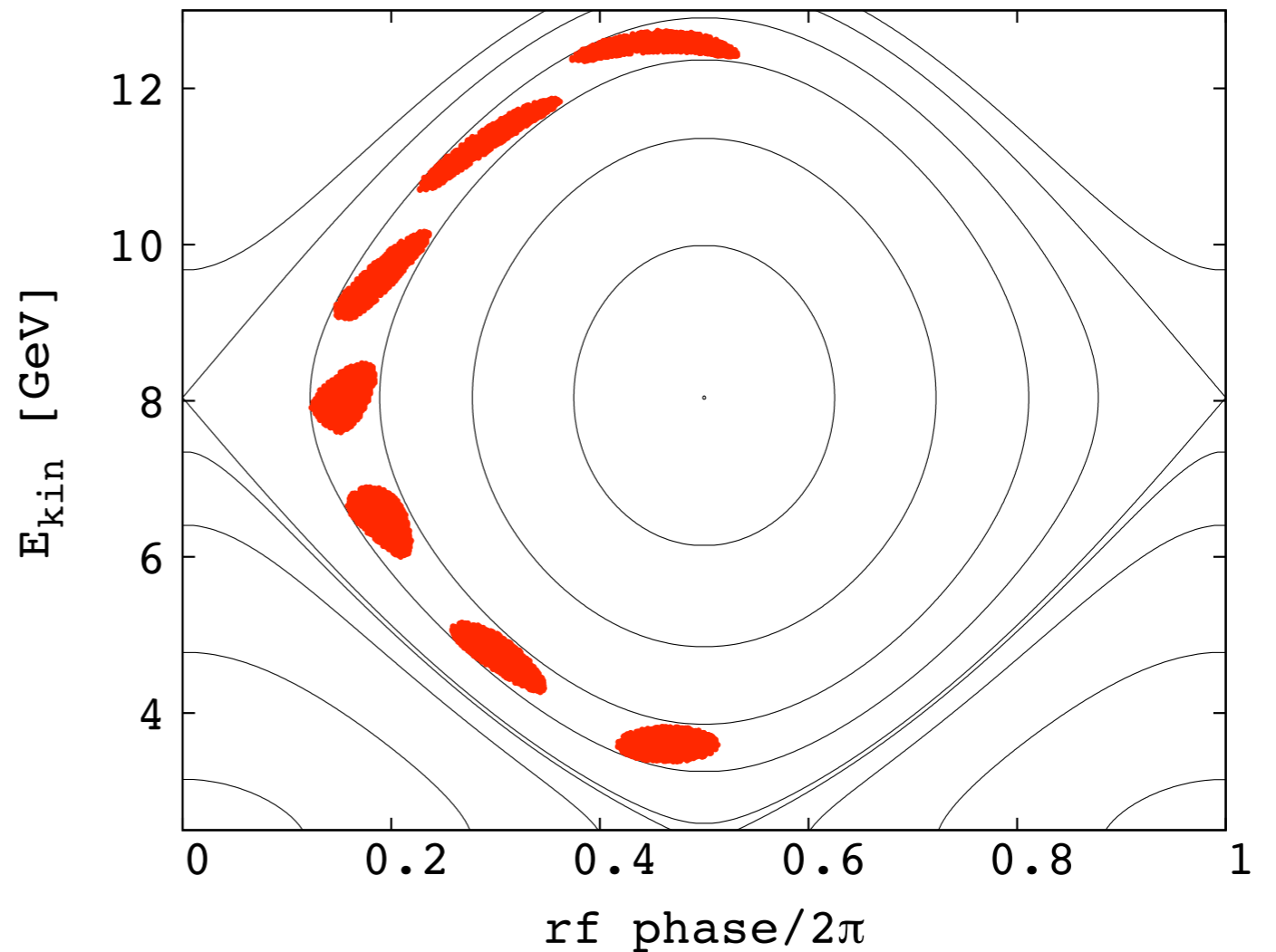
1000 particles are **uniformly distributed** inside a transverse 4D ellipsoid (Waterbag distribution); these particles are then independently distributed uniformly inside an ellipse in the longitudinal plane. Initial normalized bunch emittances are **30π mm-rad** in both horizontal and vertical planes and **150 mm** in the longitudinal plane.

Full acceleration cycle - 6D tracking

- Tracking results -



Figures 8 - Initial (blue) and final (red) particles distribution in the horizontal (top), and vertical (bottom) phase space.



Figures 9 - longitudinal phase space plot showing a 6-turn acceleration cycle. Hamiltonian contours are superimposed.

Full acceleration cycle - 6D tracking

6D tracking results:

- No beam loss.
- No significant transverse emittance degradation.
- No significant longitudinal emittance degradation.
- Efficient use of the rf!

Study with errors

We consider two types of errors, in the form of:

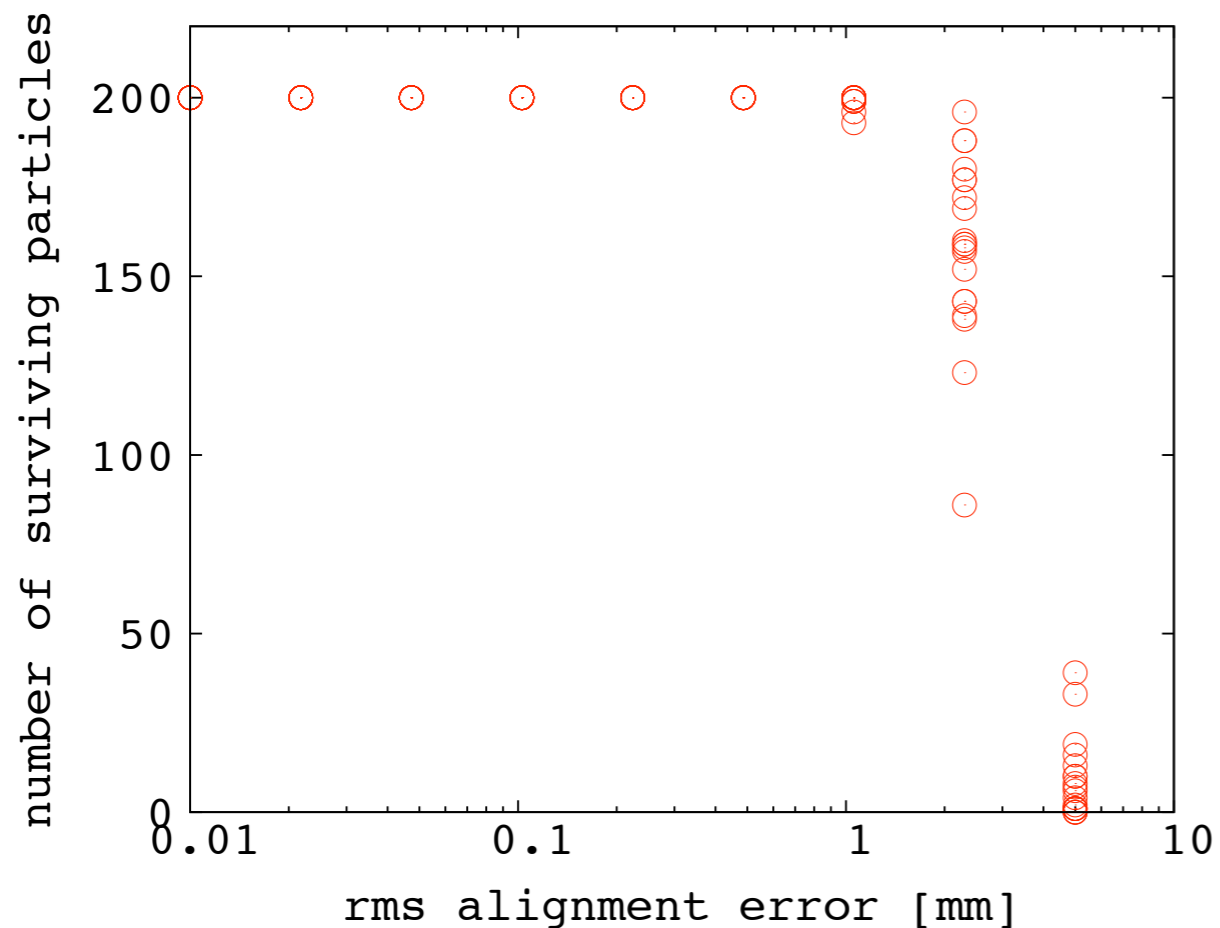
- (i) **translation** of each triplet cell,
- (ii) **rotation** around an axis passing by the triplet center.

The direction of the translation or rotation axis is randomly and uniformly chosen in the 3D space. The amplitude of the displacement is chosen following a Gaussian distribution with null mean.

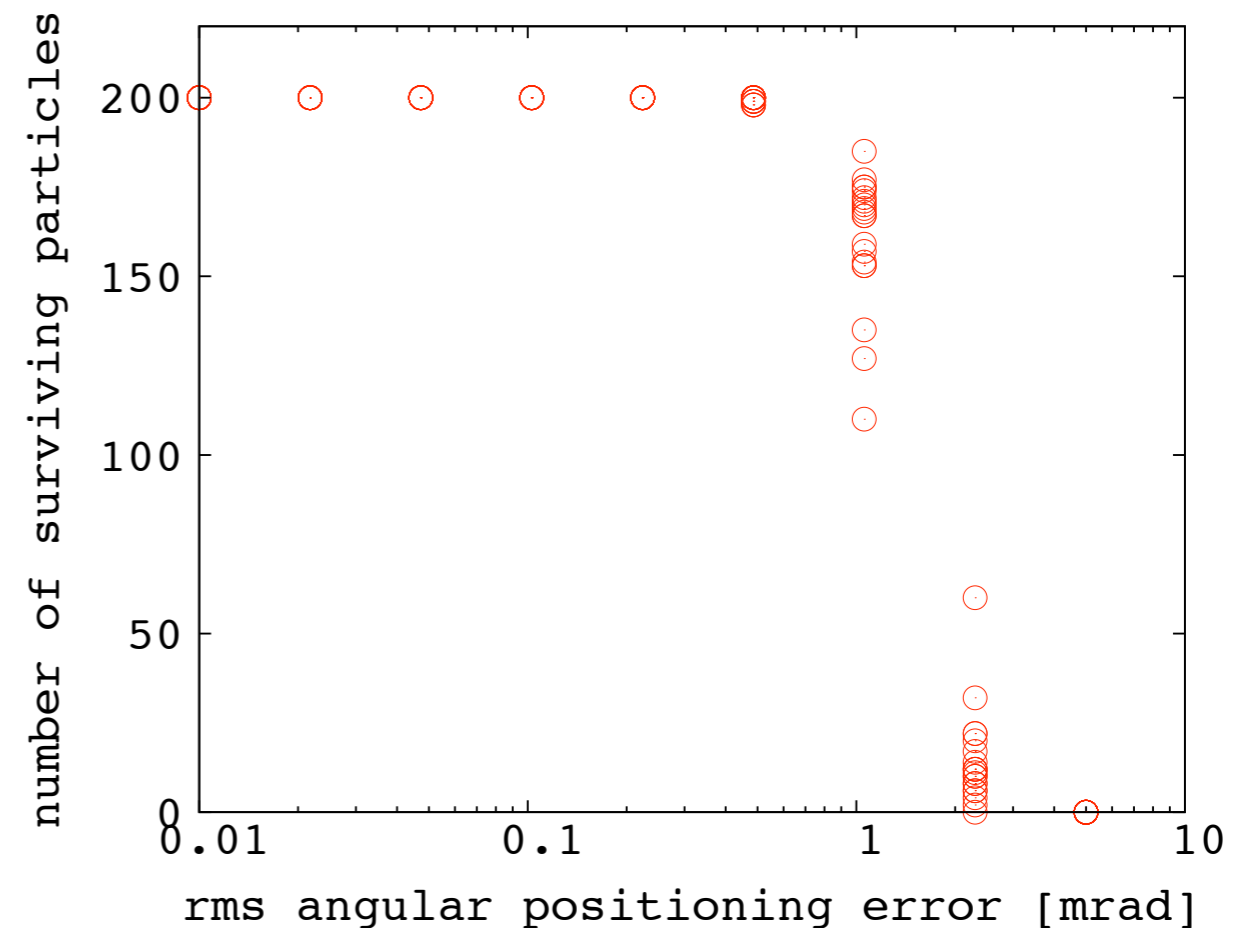
200 particles are tracked over a whole acceleration cycle (6 turns). Collimators placed in the middle of every long straight section to stop particles going at $160.7 < r < 161.1$ m, and $|z| > 90$ mm.

Study with errors

Errors in translation



Errors in rotation

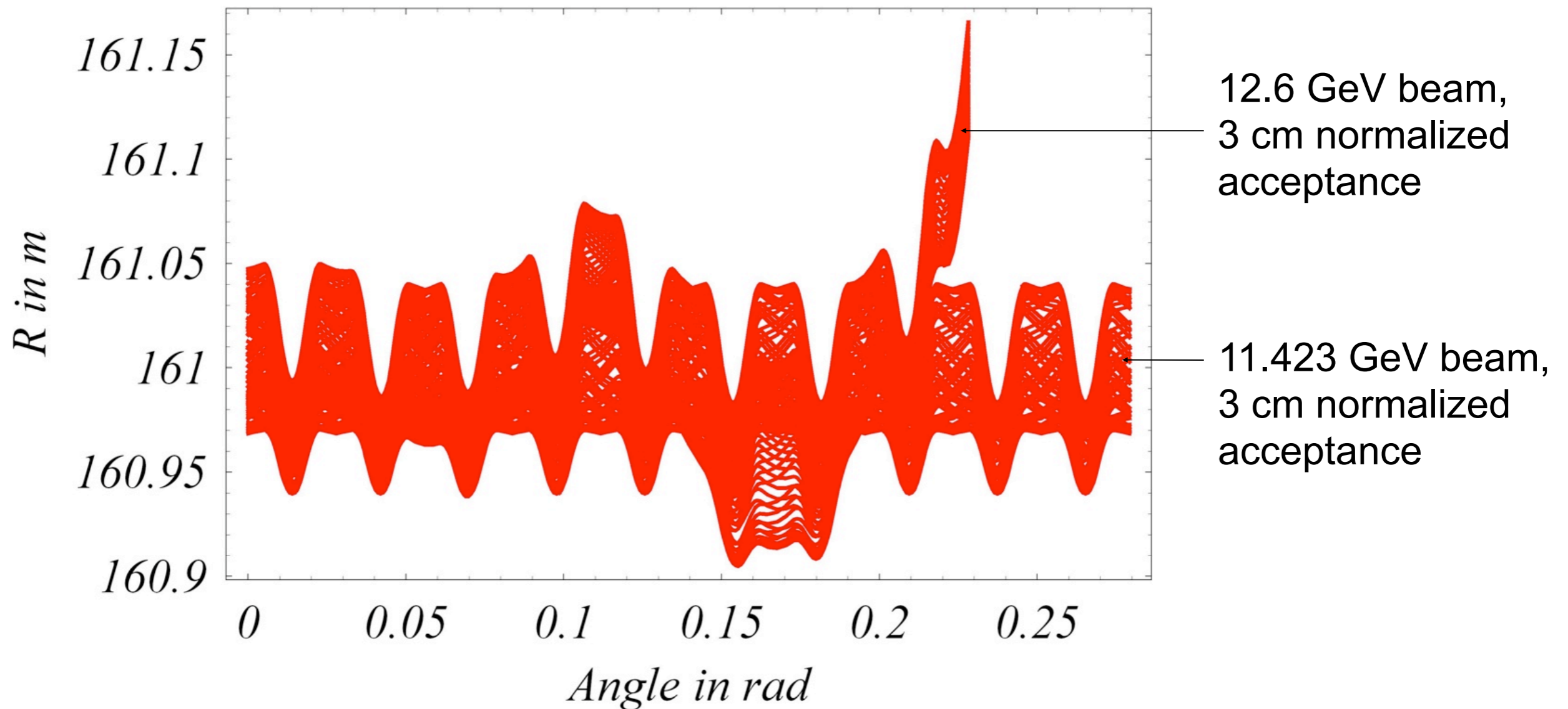


Figures 10 - Number of surviving particles depending on the rms error. 20 different lattices have been generated and tested for each value of rms error.

More tolerant to errors than the NS-FFAG!

Preliminary horizontal beam extraction

(from J. Pasternak, Imperial College London/RAL STFC)



- 4 main kickers 0.2 T, 0.96 m (0.3 m space between the kicker and the magnet)
- 3 correction kickers (sitting between main kickers) (0.0345, -0.145, and 0.12 T)
- Beam separation about 1 cm
- Septum 0.96 m, 4 T, beam separation of about 8 cm at the magnet.

Summary

Many advantages:

- Large 6D acceptance and no emittance degradation.
- Simple scheme : only one type of cell.
- Good tolerance to errors.
- Relatively compact: 1 km in circumference.
- Efficient use of the rf cavities: **6 turns** with this design,

Still to be done:

- Injection/extraction,
- Detailed magnet design,
remarks: (i) we assumed $< 4\text{T}$ max, small beam size (very strong focusing), relatively small excursion ($< 15\text{ cm}$). (ii) Research program on superconducting FFAG magnets already approved will start at Kyoto University. (iii) Combined function magnets used in the neutrino beam line at J-Parc look very much like^(*).

^(*) see T. Nakamoto et al. , Transactions on Applied Superconductivity, vol. 15-2, (June 2005).

Thank you!

Appendix:

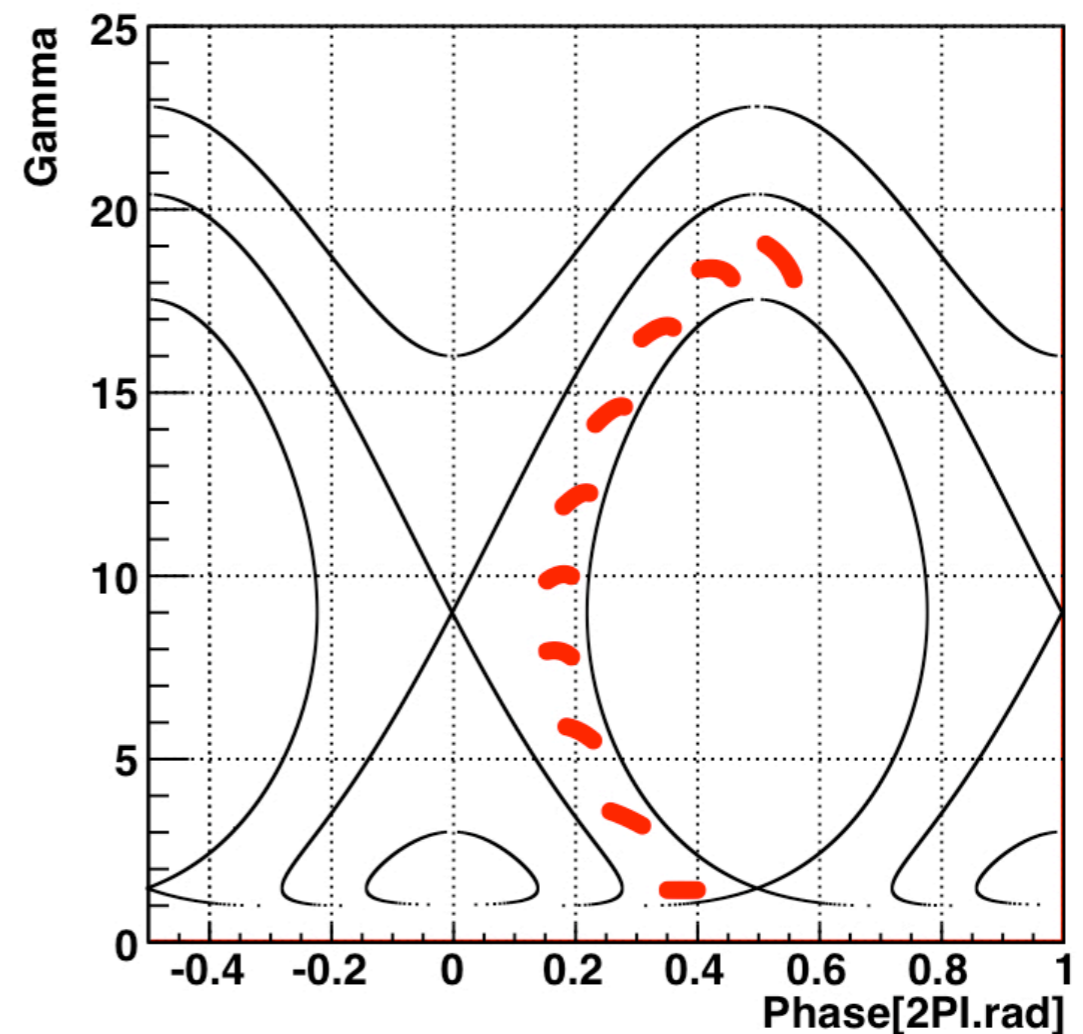
And this is not all what we
can do for muon acceleration
with scaling FFAGs!!

Acceleration between rf buckets

(slide from E. Yamakawa, look at the proceedings of FFAG'09 for all details)

Injection phase	0.35-0.4 2π rad
Injection Kinetic Energy @ $\phi=0.375$ 2π rad	44-45 MeV
Final Kinetic Energy @ $\phi=0.5$ 2π rad	1805-1905 MeV
Stationary Kinetic Energy @under E_t	844.8 MeV
k 值	6
Mean Radius @ γ_s	10 m
V_{RF} / turn	250 MV
F_{RF}	4.7 MHz
Number of cavity	10
Number of turn	9 turn

Example of ~40 MeV to ~1.85 GeV muon scaling FFAG ring parameters.

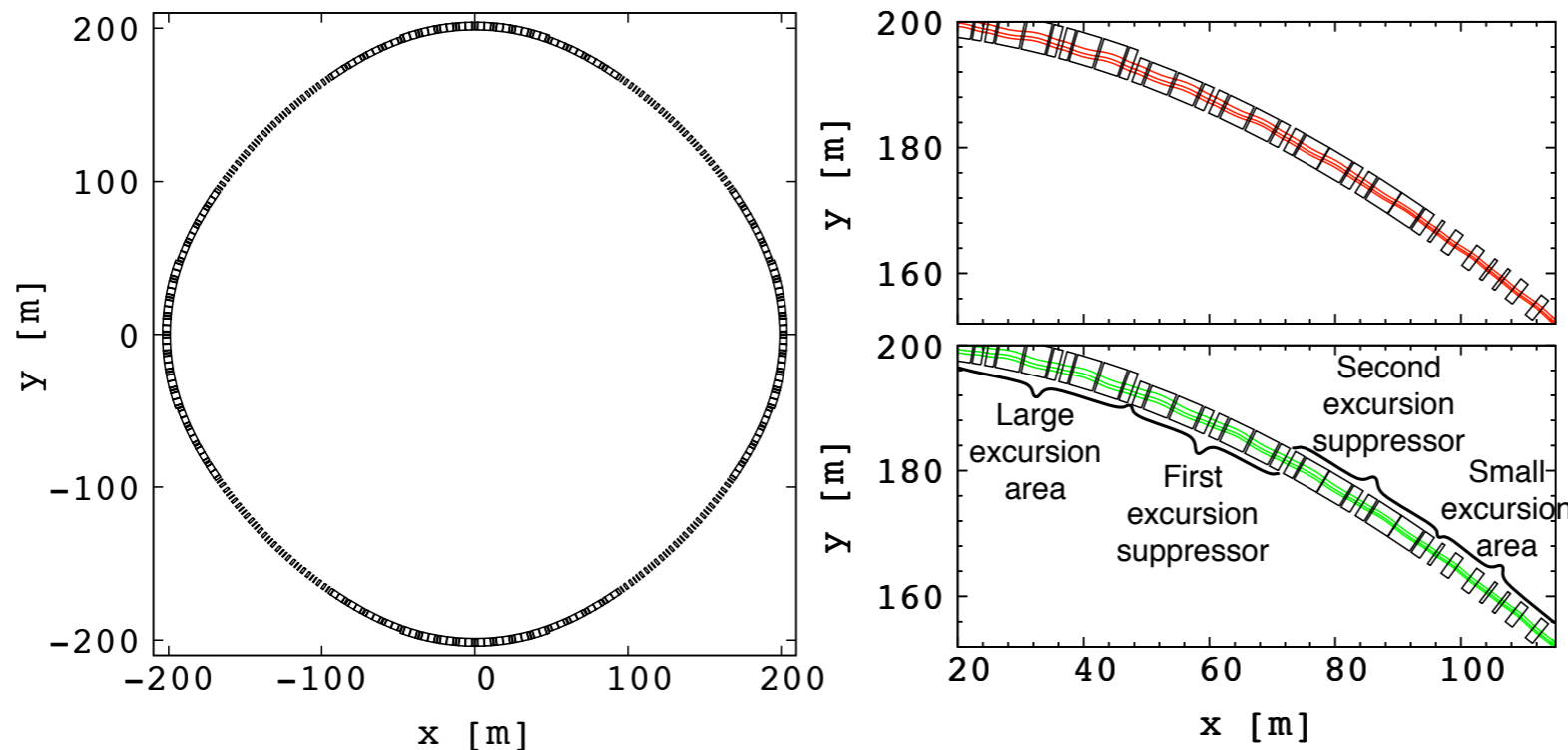


Longitudinal phase space plot showing a 9-turn acceleration cycle. Hamiltonian contours are plotted in black.

Using harmonic number jump acceleration

We recently proposed a 3.6 to 12.6 GeV lattice made of scaling FFAG cells using ~400 MHz rf frequency (see proceedings of FFAG'09 for all details). In few words:

- Cavity are placed in excursion reduced insertions.
- Both μ^+ and μ^- beams can be accelerated simultaneously.
- Large 6D acceptance has been confirmed by tracking.



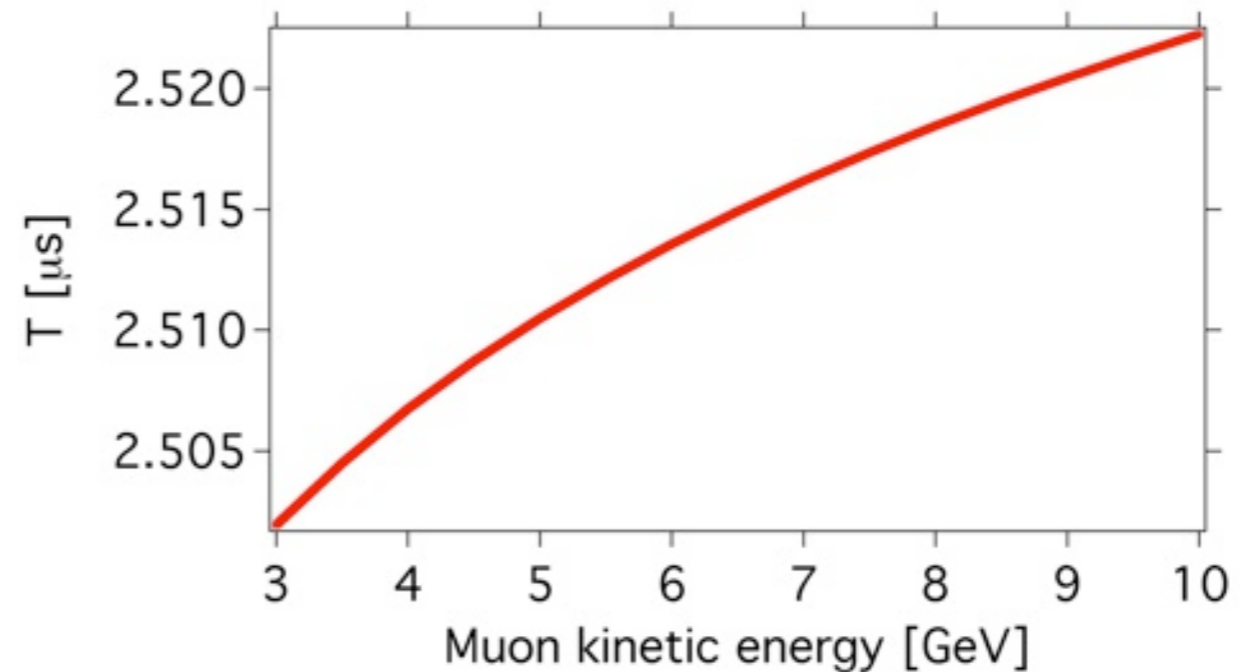
Figures A2 - Schematic view of a 3.6 to 12.6 GeV muon ring, made of scaling FFAG cells, with excursion reduced insertions.

This scheme is not as simple and as compact as the ring for stationary bucket acceleration. Could be preferable for acceleration from lower energies.

Principle and constraints of the HNj acceleration

To jump one harmonic every turn: $T_{i+1} - T_i = \frac{1}{f_{rf}}$

Figure A3 - Revolution time as a function of particle energy in the case of a 3 to 10 GeV scaling FFAG ring, with $k = 145$ and average radius = 120 m.



➔ Energy gain per turn must follow: $\Delta E_i = \frac{1}{f_{rf} \cdot \left[\frac{\Delta T}{\Delta E} \right]_{E_i}}$


Principle and constraints of the HNj acceleration

Need for dispersion suppressor insertions:

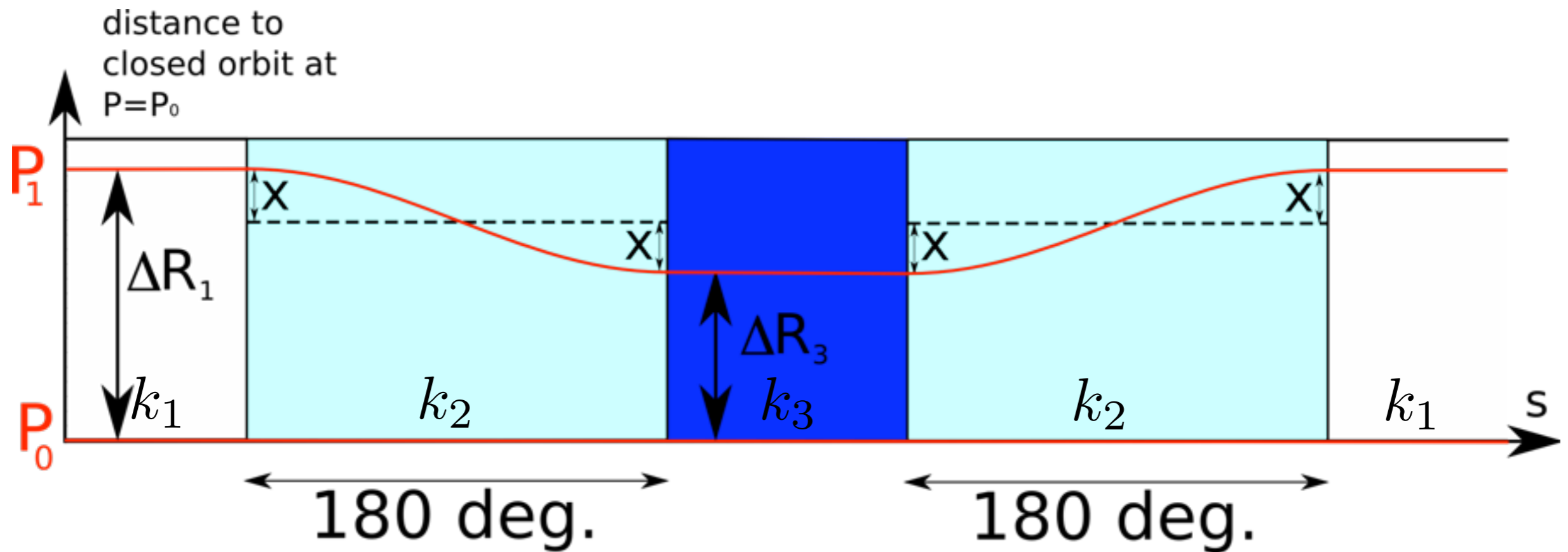
Harmonic jump condition: $T_{i+1} - T_i = \frac{1}{f_{RF}}$

In the same time: $\frac{\Delta C_i}{\beta c} = T_{i+1} - T_i$

In case of highly relativistic particles: $\Delta R_i \approx \frac{c}{2\pi f_{RF}} = \frac{\lambda_{RF}}{2\pi}$

average excursion = $\lambda_{RF} \cdot \frac{N_{turns}}{2\pi}$  **Need for excursion reduced areas!**

Dispersion suppressor with FFAG magnets



with
$$\frac{2}{k_2 + 1} = \frac{1}{k_1 + 1} + \frac{1}{k_3 + 1}$$

Principle and constraints of the HNj acceleration

Need for a double beam lattice:

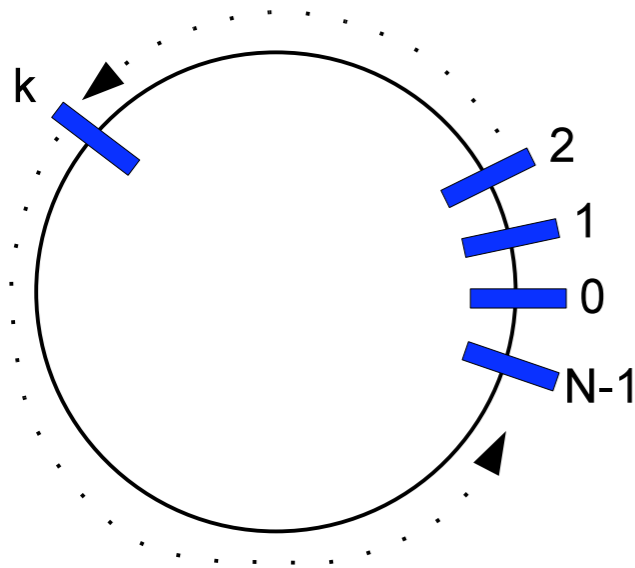


Figure A5 - N cavities homogeneously distributed around the ring.

Assuming that the initial number of harmonic h_0 is large we get^(*):

$$f_k \approx f_0 \left(1 - \frac{1}{h_0} \cdot \frac{k}{N} \right)$$

Every cavity working at a constant frequency f_k but the frequency has to be tuned to a slightly different value!

μ^+ and μ^- beams cannot be accelerated simultaneously if they circulated in opposite directions...

^(*)look at the proceedings of PAC'09 for all details.

Appendix - 3.6 to 12.6 GeV muon ring using harmonic number jump acceleration

Use of quadruplet type of two-beam scaling FFAG cells:

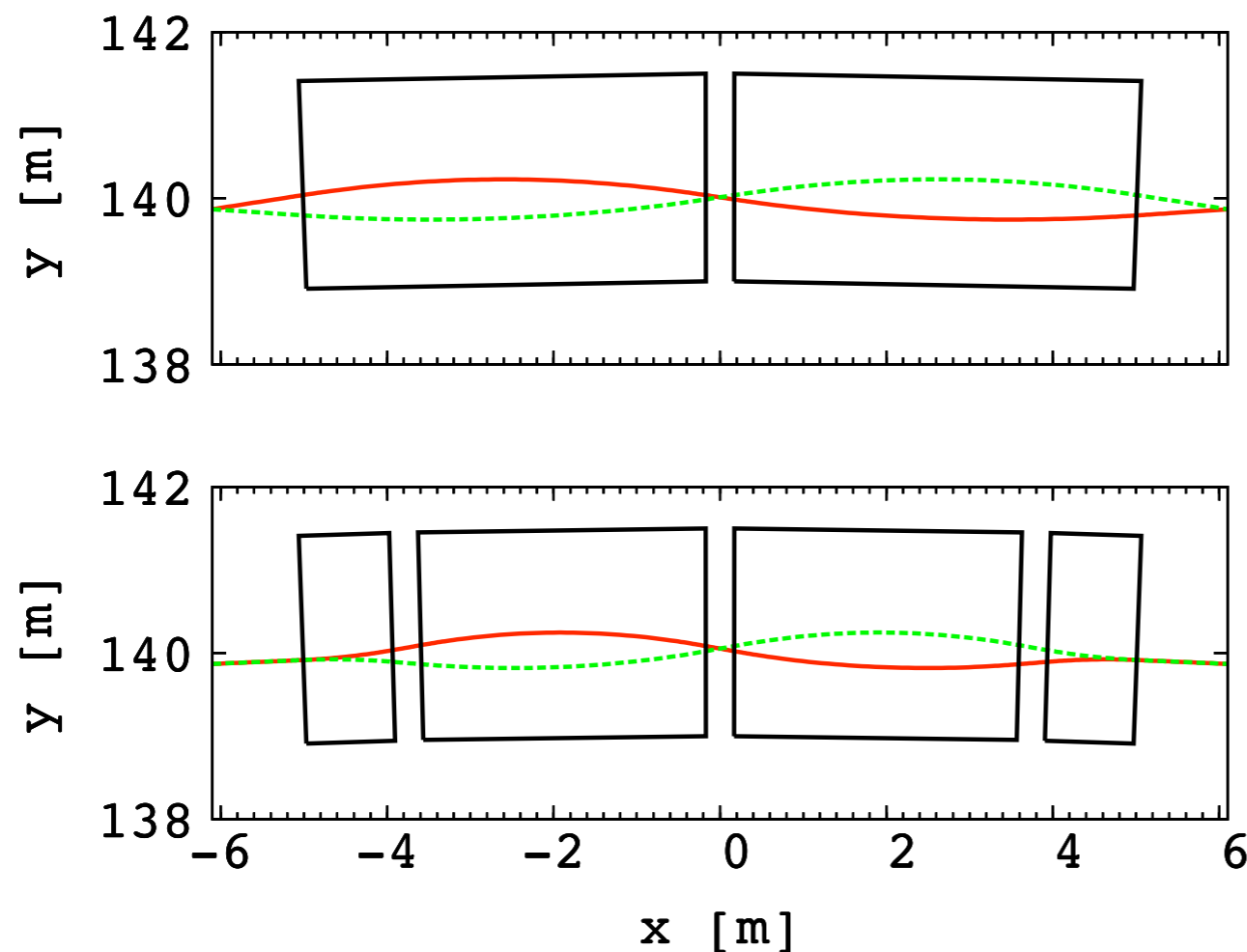
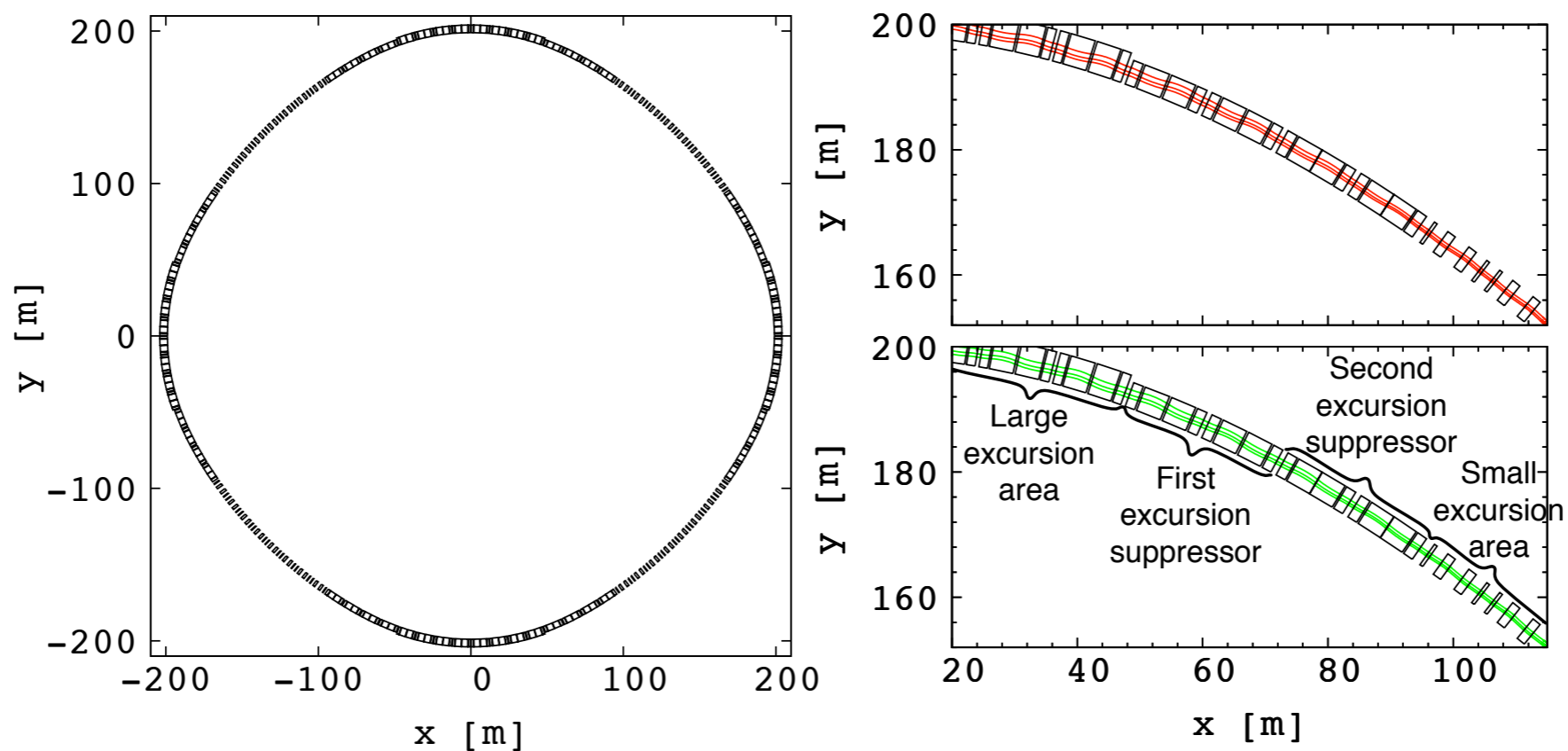


Figure A6 - Closed orbit of μ^+ and μ^- beams circulating in the same direction in a two-beam doublet (upper part) and quadruplet (lower part) scaling FFAG cell.

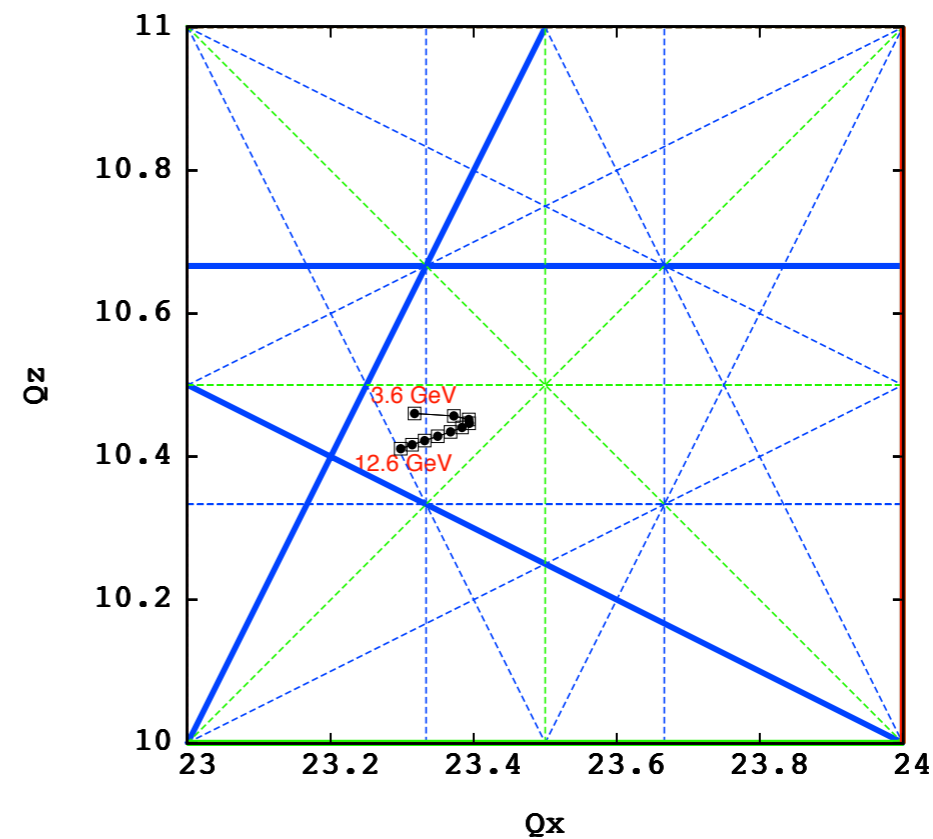
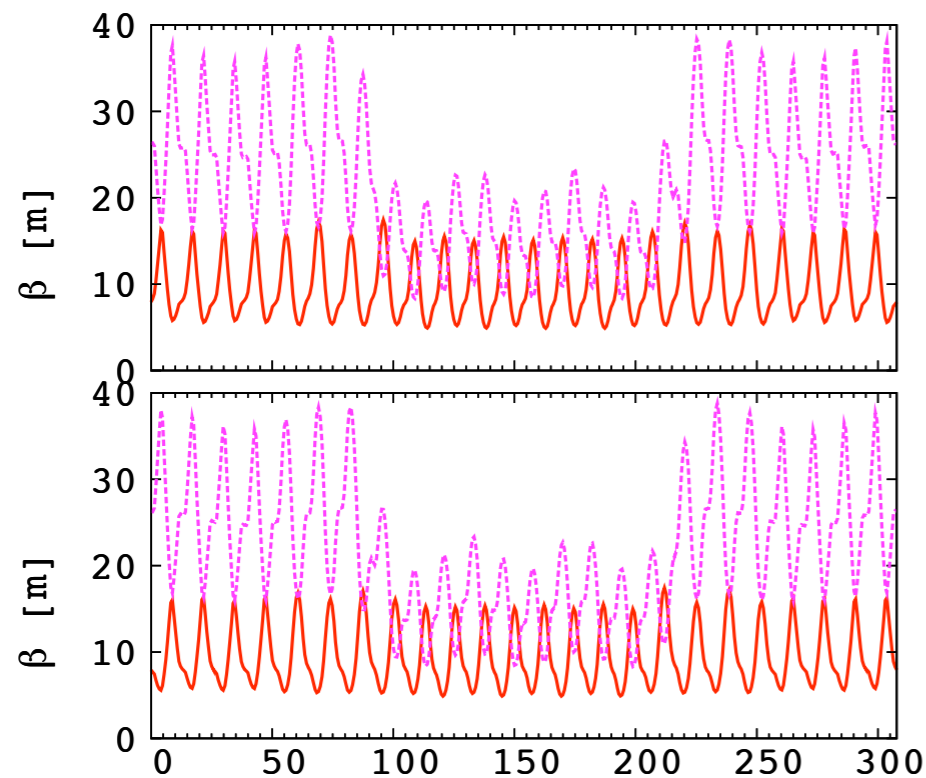
Appendix - 3.6 to 12.6 GeV muon ring using harmonic number jump acceleration

	Ring main part	Reduced excursion section	First dispersion suppressor	Second dispersion suppressor
Cell opening angle [deg.]	5	2.5	4.3	3.2
Mean radius [m]	140	295	178	240
Field index k	130	508.5	186.4	339.6
Horizontal phase adv./cell [deg.]	87.4	85.8	90.0	90.0
Vertical phase adv./cell [deg.]	50.7	30.1	42.4	31.4
Number of these cells in the ring	8×4	8×4	4×4	4×4

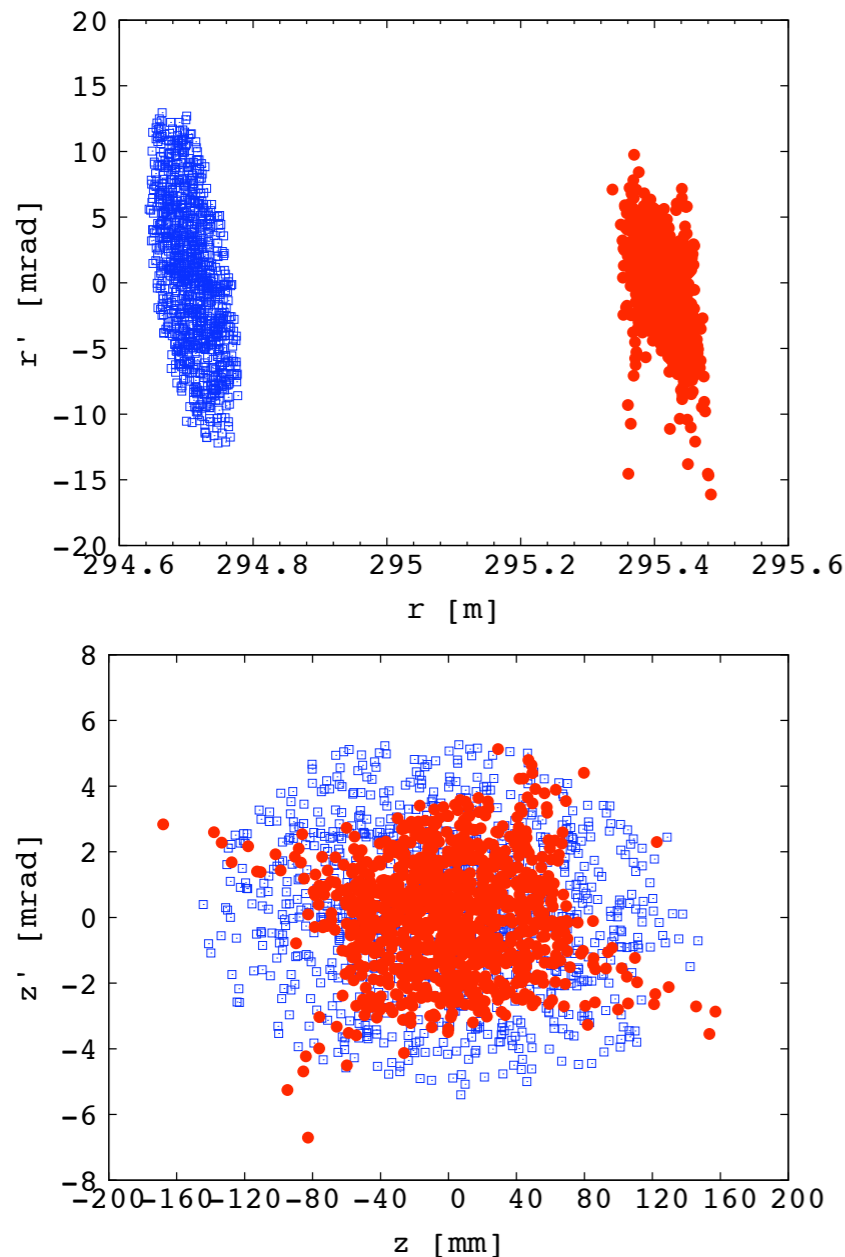


Appendix - 3.6 to 12.6 GeV muon ring using harmonic number jump acceleration

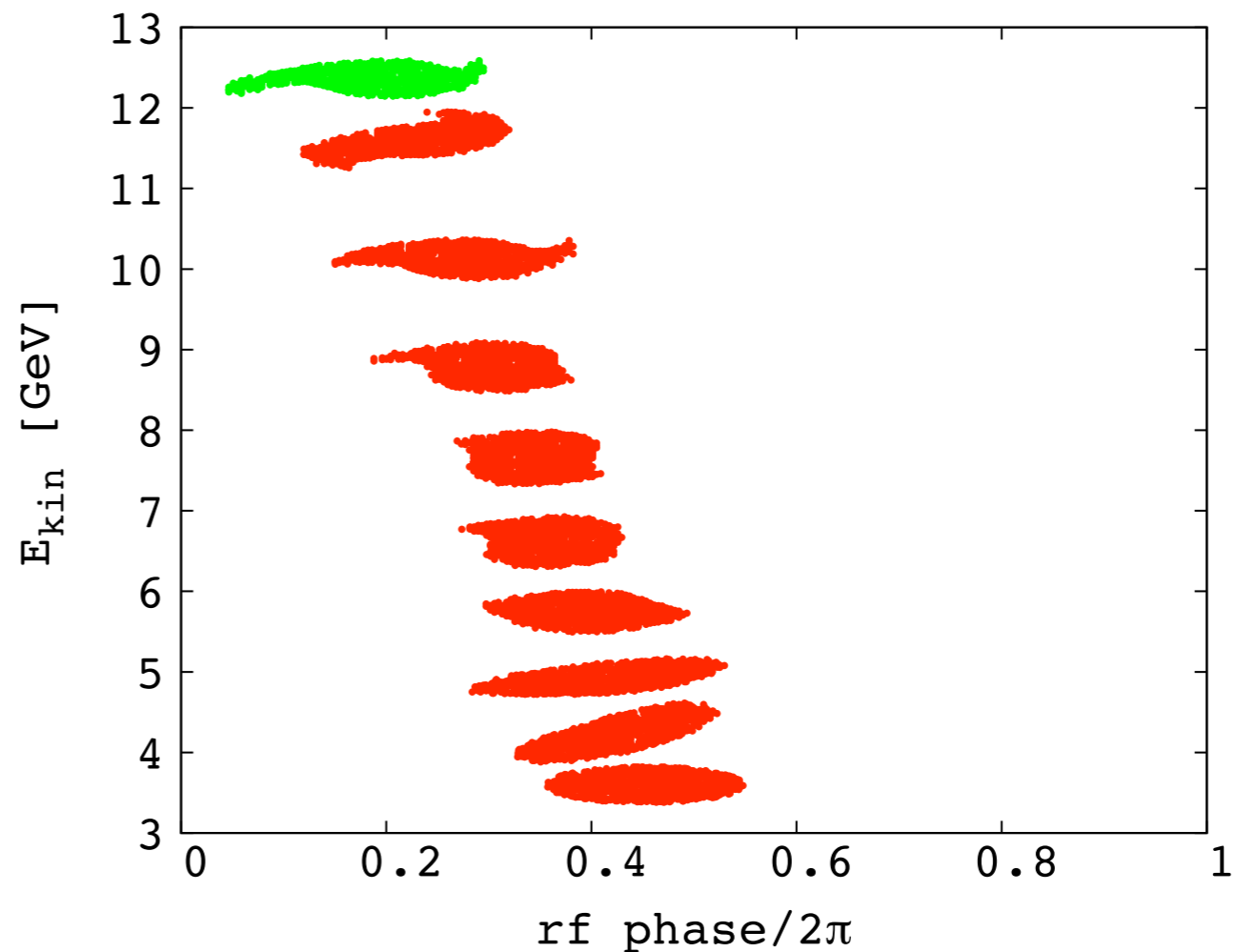
	Ring main part	Reduced excursion section	First dispersion suppressor	Second dispersion suppressor
Cell opening angle [deg.]	5	2.5	4.3	3.2
Mean radius [m]	140	295	178	240
Field index k	130	508.5	186.4	339.6
Horizontal phase adv./cell [deg.]	87.4	85.8	90.0	90.0
Vertical phase adv./cell [deg.]	50.7	30.1	42.4	31.4
Number of these cells in the ring	8×4	8×4	4×4	4×4



Appendix - 3.6 to 12.6 GeV muon ring using harmonic number jump acceleration - 6D tracking results -



Figures A9 - Initial (blue) and final (red) particles distribution in the horizontal (top), and vertical (bottom) phase space.



Figures A10 - longitudinal phase space plot showing a 8.5-turn acceleration cycle. rf frequency = 400, sum of the rf peak voltage over one turn = 2.1 GV.